EFFECTS OF OPERATING VARIABLES OF RED MUD DEEP THICKENING

by

(C) Jacqueline M. Cameron, B.Sc. Eng. (U.W.I.)

A Project Report

Submitted to the Faculty of Graduate Studies

in Partial Fulfilment of the Requirements

for the Degree

Master of Engineering

McMaster University

June 1980

MASTER OF ENGINEERING (1980)
(Chemical Engineering)

McMASTER UNIVERSITY
Hamilton, Ontario

TITLE: Effects of Operating Variables of Red Mud Deep Thickening

AUTHOR: Jacqueline M. Cameron, B.Sc. Eng. (University of the West Indies)

SUPERVISORS: Dr. D. R. Woods, Mr. D. Noteboom

NUMBER OF PAGES: xiii, 144

ABSTRACT

The effects of operating variables of red mud deep thickening have been examined. The independent (operating) variables studied were 1) The dosage of an anionic polymeric flocculant and 2) the solids throughput. The dependent variables were the concentration of underflow solids, underflow withdrawal rate, overflow rate, overflow quality and steady state solids concentration profile.

The major effect of the flocculant dose was an increase in the separation efficiency (a measure of the degree of thickening) for an increase of flocculant dose.

The solids concentration profiles obtained showed that the majority of the thickening of the mud occurred in the bottom fifth of the column. Therefore, for a given thickener and mud type, there exists a certain bed depth above which no substantial gain in separation efficiency is achieved.

When all other variables are the same, the column diameter-to-length ratio and operational temperature had the most significant effect on the separation efficiency.

ACKNOWLEDGEMENTS

I wish to express my sincere appreciation to my supervisors, Dr. D. R. Woods, Mr. D. Noteboom, Dr. G. Fulford and Mr. S. Ostap for their guidance and helpful suggestions during this work.

I would also like to thank others who contributed to this project:

Dr. P. McGeer, Mr. J. Winch and Mr. R. Pallen who made arrangements for me to undertake the graduate internship program with Aluminum Co. of Canada Ltd.;

MM. L. Lépine and G. Boulianne who expedited completion of the research;

The technical staff at the Alcan Arvida Research Centre, especially MM. Y. Brassard, R. Couture, R. Simard, C. Tremblay and P. Fortin;

Mme. M. Paradis for excellent typewritten reports during my sojourn at the Alcan Arvida Research Centre;

Aluminum Co. of Canada Ltd., not only for providing financial support for the research but also for permitting the release of information;

Finally, Ms. Linda Hunter, whose accurate typing was very much appreciated.

TABLE OF CONTENTS

LIST OF TABLES

LIST OF FIGURES

CHAPTER 1

INTRODUCTION

A thickener is a device which uses gravitational force to effect a solid-liquid separation. It is used in Bayer process plants primarily to recover caustic soda. As the particles are finely divided, a pretreatment step is required to increase the particle size, thereby resulting in a faster settling rate of particles. Polymeric flocculants are widely used in this step.. The aggregates resulting from this treatment exhibit compressible behaviour, even more so than particles which aggregate naturally.

This plastic nature of polymer flocculated sludges have led to thickeners designed to take advantage of the solids stress to obtain a thicker underflow. In the bauxite processing industry, it is extremely important to discharge as thick a slurry as possible to the mud lake for the following reasons:

(1) Protection of the environment,

(2) Increased life of the lake, and

(3) Recovery of greater quantities of caustic liquor.

Although many researchers have mentioned the importance of the flocculant in the thickening of polymer assisted flocs, very few have investigated the effect that the flocculant dosage has on

the solid-liquid separation. Therefore, the aim of this research was to study the effect of flocculant dosage and solids throughput on the separation efficiency of red mud slurry. The main apparatus used in the investigation was a 11.6 m (38 ft.) high, 10.2 cm (4 inches) wide column. It was built this high to provide a large solid stress when filled with slurry and the size of the diameter was chosen for economic reasons.

CHAPTER 2

LITERATURE REVIEW

In this thickening review, the thickening characteristics of particulate and flocculent suspensions are compared. Then, the relation between the thickening behaviour and design procedures is shown for each type of suspension. Finally, flocculent suspensions are focussed on as most suspensions can be classified as such. The different factors influencing the design are dealt with and how present-day designers account for these in the modelling of the compression zone for design purposes is presented. Finally, the objectives of this research are outlined.

2.1 Thickening Characteristics - Particulate vs. Flocculated Suspensions

Thickening is a process used to increase the solids content of sludge by removing a portion of the liquid fraction. The thickening of slurries by gravity has been an area of major interest for a long period of time due to the economics of this separation process. The sedimentation process (with respect to thickening) depends on the solid properties, as well as solid-liquid and solid-solid interactions. On the basis of these interactions, two types of suspensions can be described:

(1) Particulate: That refers to particles which settle as individual entities with no significant interaction between neighbouring particles except through hydrodynamic mechanisms. Coarse mineral particles possess this kind of behaviour.

(2) Flocculent: That refers to particles which coalesce or flocculate during the sedimentation operation so that there is significant interaction between particles. Most materials, especially water, wastewater treatment sludges (examples of natural flocs NF) and particles flocculated with chemicals (chemical assisted flocs) are examples of this type of suspension.

Based on this classification of the type of suspension, Fitch (1962) proposed a characterization of the sedimentation process into three wide classes based on Deane's work (1920). These classes of sedimentation process are:

(1) Clarification,

(2) Zone settling, and,

(3) Compression settling.

Fitch (1962) represented these types of sedimentation paragenetically, as shown in Figure 2.1. The class of process which dominates depends on the suspension type and on the concentration. Such a classification is useful because the zone that controls the thickening process dictates what fundamentals and design considerations should be made. This classification model has been confirmed by Scott (1968b, 1968c) and Comings et al (1954) who, especially importantly for this work focussed on continuous separation of flocculent suspensions.

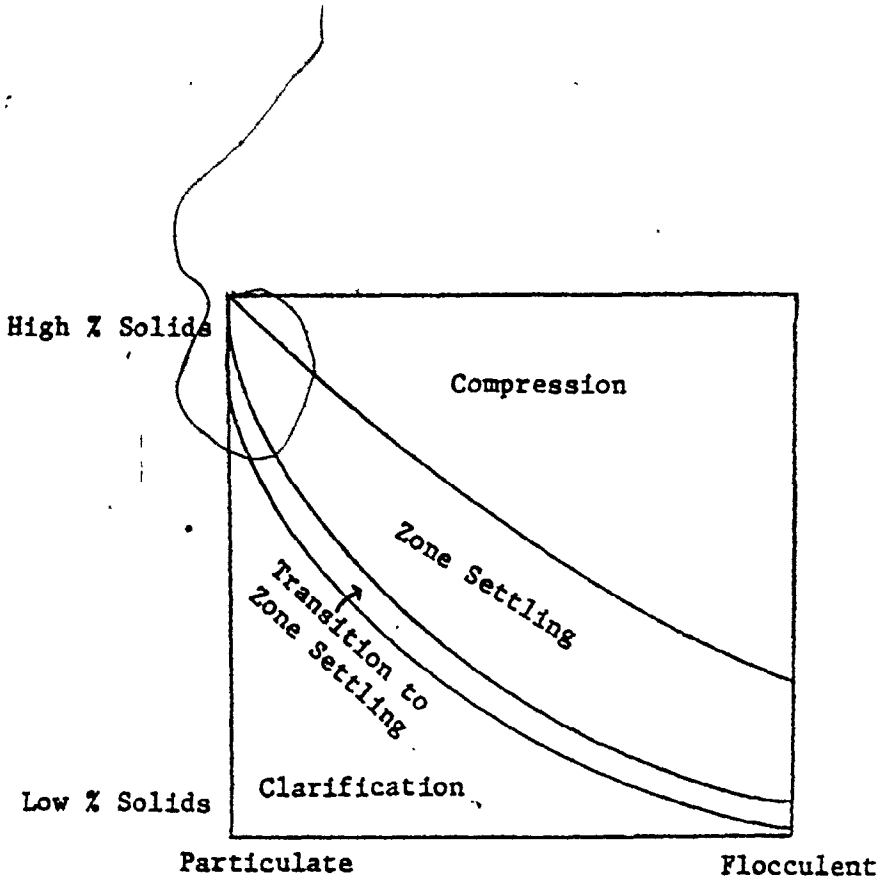

FIGURE 2-1. Sedimentation Regimes, Fitch (1962)

Although the macroscopic observations of these zones are similar for both particulate and flocculent suspensions, differences lie in the actual microscopic processes occurring in each zone. In the clarification zone, particles and/or flocs are, on the average, far apart and free to settle independently, but collisions occur. For flocculent suspensions, these collisions result in coherence while for particulate suspensions, there is no adherence. The clarification zone is often not a controlling zone as far as design or operation is concerned. In other words, if the velocity of the rising liquid is greater than the particle/floc settling velocity, then they are swept into the overflow,

but usually the design limitations based on the other zones ensures that the liquid velocity is small. Depending on the overflow quality desired for a clarification operation, this would be of importance. But clarification is not the focus of this report.

In the zone settling process (sedimentation zone), the suspension concentration is greater than that of the clarification zone. Here, particles in a particulate suspension settle as separate entities while those in a flocculent suspension aggregate as they fall to the thickening (compression) zone.

In the compression zone, the particulates or the flocs are in point contact. For particulate suspensions, the weight of particles is borne solely by hydraulic forces.

For flocs, their weight is borne partially by hydraulic forces and partially by the flocs themselves which exert a compressive force on the structure.

2.2 Design Procedures

For different types of suspensions, normally the controlling zone in the process is different. For example, in particulate suspensions, the controlling zone, which determines the design procedure used, is the zone settling region. On the other hand, in the sedimentation of flocculent suspensions, both the zone settling and compression regimes are important.

2.2.1 Particulate Suspensions

From the previous discussion, we note that there are three zones in a thickener. The suspension behaviour may be critical in one, two, or all three zones. The design of any device is usually based on some critical or controlling behaviour within that device. For particulate thickeners, the critical factor is the settleability of the suspension in the zone settling region. The behaviour in the other two zones is usually not so critical. However, some volume must be allowed at the top for the clarified liquid to escape, at the bottom so that the sludge can accumulate before being withdrawn, and for the pitch of the sides such that the discharge occurs at the desired rate.

2.2.1-1 Factors Affecting Ideal Settling

The factors that affect the settleability in the critical zone and therefore the ideal behaviour according to Kynch are:

1. Particle characteristics, and
2. Fluid mechanics and liquid properties.

1. Particle Characteristics

In the zone settling region, the particles tend to settle as a mass with the displaced liquid moving up through the instertices of the particles. The settling rate in this zone is not only a function of the solids concentration but also of its characteristics. The main characteristics of interest are the shape, size and density of the particles.

The shape of particles in most zone settling theories is assumed to be spherical. But in most systems, the particles are irregular in shape, therefore the resistance acting on each particle will depend on its orientation. Thus, a "shape factor" and "equivalent diameter" should be introduced into the settling equations in order to represent real systems.

As well as the particle shape, the density and size distribution are important in the modelling of real systems. In zone settling theories, a uniformity of particle size and density is assumed in order to simplify mathematical analyses for this zone. The particle size distribution of a suspension affects the settling behaviour since the different sizes subside at various rates which gives rise to segregation of particles. The wider the size and/or density distribution, the more readily segregation occurs. Therefore, the settling velocity is not only a function of local solids concentration as was assumed by Kynch (1952).

2. Fluid Mechanics and Liquid Properties

The settling velocity of particles in a dilute suspension can be described by Stoke's Law. But at a certain concentration, Stoke's Law becomes inapplicable due to the increase in resistance to the motion of the particles and the changing suspension properties, i.e. density and viscosity because the settling behaviour of one particle interacts with that of another. The resistance enlargement is caused by the appreciable upward velocity of the displaced fluid which alters the liquid flow pattern. Also, the velocity gradients in the fluid close to

the particles are increased as a result of the change in the area and shape of the flow spaces.

As a consequence, the assumptions made in the analysis of the zone settling behaviour depend on whether the upthrust acting on the particles is determined by the density of the suspension, rather than that of the fluid. Whether or not an effective viscosity is used is specified by the particle size distribution and the fluid characteristics.

Early workers attempted to explain the sedimentation behaviour of concentrated suspensions by a modification of Stoke's equation using the suspension properties. Richardson et al (1954b) related the settling velocity of the suspension (U_P) to the Stoke's velocity (U_S) by assuming that they are dependent on the porosity (e), the ratio of the particle diameter to that of the container (d/D), and on the Reynolds number (Re). From this theory, the general relationship derived is,

$$\frac{U_P}{U_S} = e^n \qquad \text{(eqn. 2-1)}$$

where $n = f\ (Re, d/D)$

Leclair and Hamielec (1970), solved C_D the drag coefficient, as C_D (e) for concentrated suspensions. As the C_D is a function of the Reynolds number, then the settling velocity is also a function of this also. Another theoretical estimation of subsidence velocity was presented by Happel and Brenner (1973) following two general approaches:

1. The method of reflection, which includes the wall effect.

2. The cell model where liquid is assumed uniformly distributed around each sphere. Wall effects are neglected.

The following results have been obtained by the method of reflection:

$$\frac{U_P}{U_S} = \frac{1}{1 + K\phi^{1/3}} \qquad \text{(eqn. 2-2)}$$

where U_P = actual settling velocity

U_S = Stoke's terminal velocity

K = 1.91 for cubic packing

= 1.79 rhombohedral

= 1.30 random

ϕ = concentration of solids = 1-e

By the free cell model:

$$\frac{U_P}{U_S} = \frac{3-(9/2)\gamma + (9/2)\gamma^5 - 3\gamma^6}{3 + 2\gamma^5} \qquad \text{(eqn. 2-3)}$$

where γ = a/b

a = Radius of particle

b = Radius of free cell

Maude and Whitmore (1962) correlated theirs as well as others experimental data with an equation of the form:

$$\frac{U_P}{U_S} = (1 - \phi)^{\beta} \qquad \text{(eqn. 2-4)}$$

where $\beta = \alpha/m$

α is determined by the material

m = 1 in laminar region

= 2 in turbulent region

The preceding applies to both small and large scale thickeners. But of particular importance for large scale circular thickeners is the presence of circulatory currents as it is assumed in the analysis of sedimentation that these currents do not exist. However, Chandler (1976) has shown the existence of these currents in the free settling zone (clarification zone) of a circular settler. The pattern of this current is demonstrated in Figure 2-2.

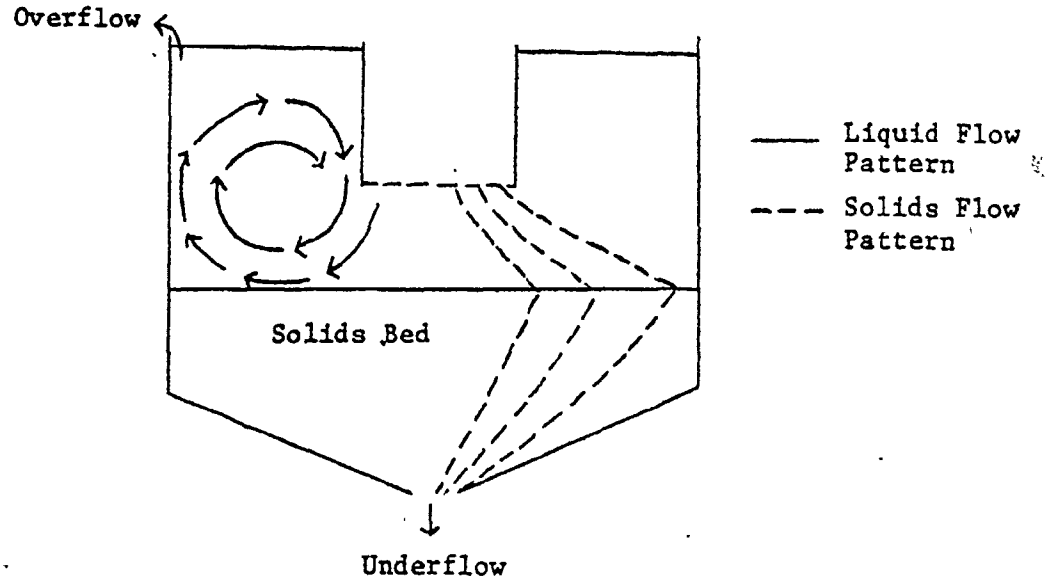

FIGURE 2-2. Liquid and Solids Flow Pattern from Chandler (1976)

This phenomenon was explained by the pressure differential set up by the higher density feed slurry falling into the lower density clarified liquid. The presence of these currents will result in a varying solids concentration across horizontal layers in this zone which makes Kynch's theory less applicable because his assumption of constant concentration across these layers is no longer true.

2.2.1-2 Design Methods

The design methods for particulate thickness are based primarily on an area evaluation for the zone settling regime; this being the critical zone. Coe and Clevenger (1916), when calculating thickener areas, introduced the use of solids-handling capacity determined by multiple batch-settling tests. Kynch in 1952 presented an analysis of settling phenomena based on a couple of assumptions: (1) the concentration is the same across any horizontal layer, (2) the settling velocity of a particle in a suspension is only a function of the particle concentration in its neighbourhood and is not influenced by concentrations of layers above or below it. Three theorems were deduced from his model.

This analysis by Kynch has been used as the groundwork for thickener design. But there have been two different methods of approach: one based on settling velocity of particles, and the other based on particle flux.

Talmage and Fitch (1955) in the design of thickeners used the Kynch analysis of constant concentration layers. They demonstrated that the function for settling velocity $u = f(c)$ can be obtained from one

batch settling curve as well as from multiple batch-settling tests. From the graphical construction of the interface height as a function of time, the time required for the formation of a given underflow concentration can be determined. Then, the necessary thickening area is calculated using the graphically specified time value.

The definition of particle flux is mass of solids passing through an area of unit cross section in unit time. Composite flux curve (showing solids flux vs. concentration) methods developed by Hassett (1958a,b,c) and Yoshioka (1955) are also used in determining thickener areas. The composite flux curve takes into consideration the discharge rate of the underflow solids in a continuous thickener and in so doing predicts the maximum handling capacity (equivalent to minimum flux). The development by Hassett (1964) to ascertain the minimum flux is more tedious than the Yoshioka (1955) method.

2.2.1-3 Summary of Design Methods

To determine the area of a thickener, the function $u = f(c)$ obtained from multiple batch-settling tests or from the Talmage-Fitch (1955) single batch settling test commonly is used with Coe and Clevenger's (1916) equation or with graphical methods of flux developed by Hassett (1958a,b,c) or Yoshioka (1955). These methods focus on the fluid/solid particle behaviour at the clarification - zone settling interface. Other methods for designing thickeners depend upon calculating the depth of the thickener from empirical methods.

2.2.2 Flocculent Suspensions

The design methods for particulate suspensions ignored the role played by depth in the compression zone. These methods are valid only for the sedimentation zone where the flocs exist individually. When sizing thickeners for flocculent suspensions, both the sedimentation process in the sedimentation zone (zone setting regime) as well as the consolidation process in the compression zone should be considered. Capacity limitations in a continuous thickener are usually connected with the compression zone, rather than the free settling zone. This view is supported by Comings (1940), Dixon (1977b) and Kos (1977). Presently, as stated by Kos (1977), there is not a simple dependable test procedure for thickening zone area and depth evaluation.

Flocculation is employed to increase the settling rate of very finely sized suspensions, therefore resulting in a smaller area demand. The efficiency of adsorption of flocculants has been shown to affect the settling rate of suspensions as reported by Tomalin (1938) and Chakravarti and Dell (1969). The efficiency of adsorption also affects the rheological properties of the sediment since the specific surface area changes.

Flocculated sediments tend to be more compressible compared with non-flocculated sediments which are more rigid. The degree of compressibility is more noticeable the more extended the polymer chain of the flocculant. Evidence of this behaviour has been reported by Couche and Goldney (1959), Scott (1965a), Shannon and Tory (1966) and Adorján (1975).

2.2.2-1 Factors Affecting Consolidation

The methods of area design, based on the function u = f(c) and the assumption of ideal slurries do not apply to the compression zone of a thickener processing flocculent suspensions. According to Dell and Keleghan (1973), the following factors besides the solids concentration have been shown to affect the consolidation rate:

1. Particle - interparticle behaviour,
2. Fluid mechanics, liquid properties, and,
3. Flocculant (type, dosage, pH, place and method of addition).

1. Particle - Interparticle Behaviour

Flocculated sediments usually consist of minute particles which are bridged by polymer molecules forming extended networks of particles held loosely together throughout the bed. Synthetic polymer flocculants tend to form more extended networks. This imparts a plastic nature to the sediment, therefore making it more sensitive than normal flocs to pressure from above. The deformation of the floc structure is a rheological phenomenon. The sediment is considered to be in a plastic condition with a set yield point which, if exceeded, results in collapse of the structure. Since with polymer-assisted flocs, the floc structure consists of particles interconnected by polymer bridges, these portions of flocculant within the structure would collapse before the structure does. This idea will be discussed further in the flocculant subsection.

The effect of pressure on the underflow solids concentration

has been shown theoretically by Adorján (1975). But Dell and Keleghan (1973), Chakravarti and Dell (1969), Kalbskopf (1972), Adorján (1976), Stinson (1979) and others demonstrated using different methods the effect of solids pressure (a term introduced by Dell and Sinha in 1966) on the attainable solids concentration. When the solids concentration of a sludge depends on the solids pressure, it is also a function of the compression zone height since the maximum solids pressure which can be exerted is directly proportional to the amount of overlying solids. However, the depth of solids alone does not determine the solids pressure produced in operation. The compressive forces generated are also a function of the residence time of the material.

2. Fluid Mechanics and Liquid Properties

Due to compressive forces in the compression zone, the flocs collapse releasing water. This water flows upwards through the sediment by a filtration process and sometimes by means of channels - this behaviour is termed channelling. This occurrence is said to aid liquid drainage rates and it has been observed by many researchers who include Coe and Clevenger (1916), Dell and Sinha (1966), Scott (1968a), Chakravarti and Dell (1969), Harris et al (1975) and Kos (1977). Roberts (1934) reported observing channelling and mound formation at the surface of the suspension/supernatant interface. The mound formation was explained as being due to channels reaching the surface and disturbing the surface as the liquid in the channels break the surface.

Channelling has been described as a non-Darcian flow by Kos (1977) who obtained this result from steady-state gravity thickening tests. However, Michaels and Bolger (1962), Smiles (1976), Stinson (1979), Kos and Adrian (1975), and Adorján (1976) found the relationship to be a Darcian one. But these researchers used tests other than continuous steady-state ones. For example, Stinson (1979), Kos and Adrian (1975) and Adorján (1976) used modified soil testing techniques. So it is possible that these bench-scale tests may not characterize the flow occurring in a large-scale continuous thickener.

Two mechanisms have been suggested to explain channelling. Michaels and Bolger (1962) postulated a vertical shell and tube model, with all the macrovoids in the tubes. Kos' (1977) idea is similar but with varying tube diameters within the structure which are dependent upon the dynamic pressure gradient. An increase in the dynamic pressure gradient results in larger diameter channels due to wall erosion. This picture of channelling does not resemble that observed where the channels are crooked.

Fitch's (1966a) mechanism derived from flux continuity and Kynch theory, postulates that horizontal pockets of either fluid or suspension of lowered concentration will tend to segregate where the second derivative of the flux curve is positive. The horizontal strata of lowered density forces channels through to the surface if it is coherent. This mechanism explains the segregation of bubbles of

fluids sometimes observed, which is not resolved by the capillary tube model.

These mechanisms together are complimentary as one explains what the other does not. Maybe these mechanisms could be incorporated into one mechanism to explain channelling.

The foregoing postulated mechanisms attempt to describe natural channelling, however, the majority of thickeners in use incorporate mechanical devices (e.g., rakes) which gives rise to forced channelling. Couche and Goldney (1959), Comings et al (1954), Comings (1940) and Dell and Keleghan (1973) have shown that slow stirring leads to higher final densities at the bottom of the compression zone. Laboratory batch tests on flocculated red muds also clearly show that slow stirring promotes higher final solids concentration. This was believed due to the floc structure being broken up, thereby promoting the formation of escape channels for returning fluid. But this could also be due to the stirrer disturbing short circuit currents from the feed to the underflow outlet. Dell and Keleghan (1973) obtained similar solids distribution within stirred sediments compared with that predicted by vacuum filtration tests, which they attributed not only to the promotion of channelling but also the prevention of the solids structure bridging the vessel diameter. In addition to the mechanisms cited, stirring may not only open up channels within the bed but also along the stirrer device where liquid can preferentially channel upwards by a "wall" effect.

Mechanical disturbances in the form of vibrations have been shown to increase the settling and consolidation rate of flocculated suspensions. The vibration may ameliorate thickening by mechanisms similar to that proposed for stirring.

3. Flocculant

As flocculated sediments undergo compression, both the polymeric flocculant and the particles experience this pressure due to interparticle contact. As the synthetic flocculant requires less pressure to deform than the particles, it will collapse first. Therefore, the type of flocculant, how it is adsorbed onto the particles, the dosage used and the conditions of addition should have an important effect on the consolidation rate of the sediment.

Although the references studied have mentioned the importance of the flocculant in thickening, most have chosen to ignore this factor in thickening research. Dell and Keleghan (1973) have shown using vacuum filtration tests on clay suspensions that the flocculant dosage affects the permeability of the sediment but has a negligible effect on the equilibrium dewatering under applied suction. Wright and Kitchener (1976) demonstrated using "gelling" clays not only the permeability of the sediment was affected but also the strength. Bonjer and Clement (1974) made a study of the effect of flocculants on filtration rates. They found that addition of flocculant increases the cake permeability, and hence the filtration rate, up to some critical dosage. Beyond this dosage, more flocculant causes the filtration rates to decrease. An "optimum" dosage has not been

identified for thickening, though perhaps it ought to exist also.

Therefore, due to the lack of information on this area, the main concern of the deep thickening research was the influence of the polymeric flocculant on the thickening efficiency.

2.2.2 -2 Conventional Design Methods

Conventional design methods for thickeners rely heavily on the identification of the compression point because thickener areas are usually based on batch settling rates at the compression point dilution. This point is visualized as that at which the solids below the slurry-supernatant interface pass into the compression regime.

Location of the compression point can be made readily for particulate suspensions, as observed by Coe and Clevenger (1916) as a noticeable change in sedimentation rate of the clarification - zone-settling interface (curve 1 of Figure 2-3). However, with suspensions of polymer assisted flocs, PAF, and normal flocs, NF, the velocity of descent of the slurry-supernatant interface changes gradually (curve 2 of Figure 2-3). Therefore, the compression point can only be estimated. Couche and Goldney (1959) and Panov et al (1973) have put forth methods in order to fix the compression point for polymer flocculated suspensions. But these methods require subjective judgement in determining this point.

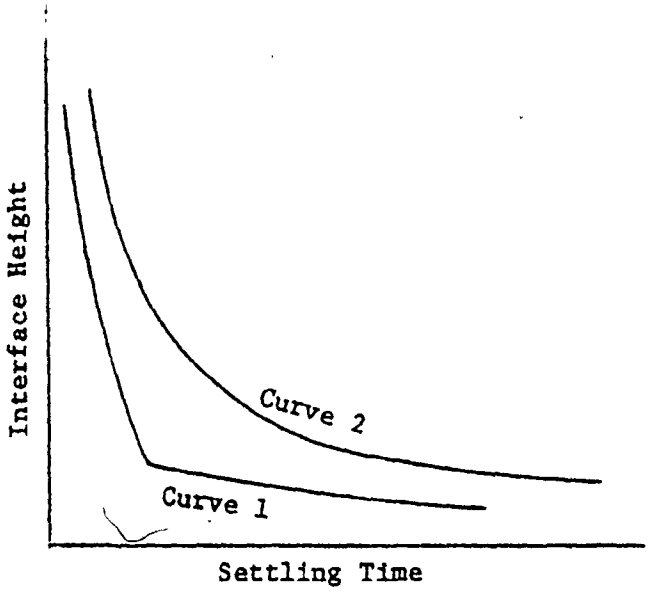

FIGURE 2-3. Typical Batch Settling Curves

The behaviour of compressible sediments is influenced by factors other than the local slurry concentration as postulated by Roberts (1949), Michaels and Bolger (1962) and Dell and Keleghan (1973). The assumptions of batch settling tests are that $u = u(c)$ and that capacity limitations only exist in the zone settling region. But capacity limitations for compressible sediments usually exist in the thickening zone. Fitch (1966b) and Dixon (1977b) maintain that they can only occur in the compression regime while Adorján (1975) states that limitation can exist in either zone. Therefore, observance of the compression point or flocculent sediments is not an accurate design method. Also, since batch sediment compression can not duplicate those occurring in a

continuous thickener, alternative design methods have been postulated. These are based on regarding the process occurring in the compression zone as a consolidation one. Therefore, the compression zone is characterized by obtaining the filtration and deformation properties of thickened materials.

2.2.2-3 Present Design Methods

Presently, design of the thickening zone for flocculated sludges center around modelling the thickening process from momentum balance equations. The models all assume one-dimensional flow, microscopically incompressible solid and liquid phases, and that all flocs in a given neighbourhood will settle at the same rate. Differences between the models lie in the assumptions made solving the force balance equations. Fitch (1979) reviews the current models for sedimentation of flocculent suspensions in the compression zone as well as the clarification and zone settling regimes. Kos (1977), Michaels and Bolger (1962), Stinson (1979) and Adorjan (1976) in deriving the momentum balance for the thickening (compression) zone considered the portion of the solids stress transmitted mechanically. However, Dixon (1978) points out that solids stress is also transmitted hydrodynamically. But the significance of this omission is presently not known.

The general equation is derived by force balance across a lamina of suspension of thickness dx and area A (Figure 2.4).

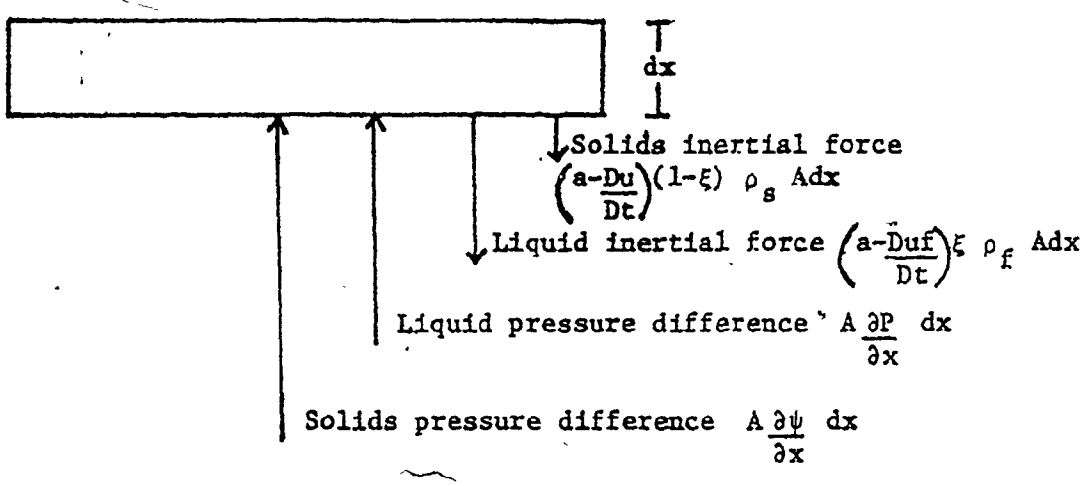

FIGURE 2-4. Thickening Force Balance, Fitch 1979

where
- a = System acceleration
- A = Settling area
- ξ = Porosity
- u = Solids settling velocity (with respect to slurry)
- u_f = Fluid velocity (with respect to slurry)
- ρ_s = Density of solids
- ρ_f = Density of liquids
- P = Fluid pressure
- ψ = Solids pressure

Force Balance:

$$\left(a - \frac{Du}{Dt}\right)(1 - \xi)\ \rho_s\ Adx + \left(a - \frac{Duf}{Dt}\right)\xi\ \rho_f\ Adx = A\frac{\partial P}{\partial x}\ dx + A\frac{\partial \psi}{\partial x}\ dx$$

(eqn. 2.5)

To solve eqn. 2.5 after the appropriate simplifying assumptions are made, empirically-determined relationships between permeability and void ratio, and also the solids pressure and porosity are needed. Initially it is assumed that the compressive stress σ, and permeability k, are each functions of solids concentration C'. Some of the empirically-fitted relationships for the solids concentration as a function of compressive stress are shown in Table 2.1. From the form of the relationships, it is seen that a certain compressive stress has to be developed before the slurry deforms (Buckingham fluid behaviour). Adorjan (1976), Stinson (1979) and Kos and Adrian (1975) determined these correlations from load cell tests which showed that σ was only a function of concentration (at equilibrium) and that Darcy's law applied for the liquid flow. In solving the force balance equation, Adorjan (1976) applied Richardson's and Zaki's (1954) empirical relationship to the compression zone. This relationship was derived for the zone settling region of a particulate suspension undergoing sedimentation, therefore, its applicability to the compression zone is questionable.

Kos (1977) estimated the constitutive relations for permeability k and compressive stress σ from steady state continuous thickening results. He discovered that not only was the permeability a function of concentration but also of the relative velocity. Therefore, contrary to load-cell tests, the liquid flow in the bed was a non-Darcian one. But Dixon (1980) using a theoretical basis has expressed doubts about Kos' (1977) results. The theoretical analysis used to question Kos' (1977) findings were based on the physical characteristic of red mud while Kos

TABLE 2-1: Empirically Fitted Compressive-Concentration Relationships

Researcher	Slurry	Polymer Type	Compressive Relationship Fitted $\sigma = \sigma(C)$
Dell and Keleghan (1973)	clay suspension	synthetic polymer	$(A_1 C')^{-1} = A_2 + A_3 \sigma^{-A_4}$
Kos (1977)	water treatment plant	not mentioned	(1) $\frac{A_5 C'}{1 + A_6 C'} = C'b + A_7 \sigma^{A_8}$ (2) $C' = C'(\sigma, T)$
Chandler (1976)	mud tailings from Bayer process	synthetic polymer	$C' = A_9 + A_{10} \lg \sigma$
Adorján (1976)	silica suspension	Magnaflox 455	$\frac{A_{11} C' - A_{12}}{A_{13} - A_{14} C'} = A_{15} \sigma^{A_{16}}$

$A_1 - A_{16}$ are constants

C' = concentration of solids as $\frac{\text{mass of solids}}{\text{mass of slurry}}$

σ = stress force/unit area

$c'b$ = solids concentration in top layer of bed

T characterises flow conditions

(1977) experimented with water treatment plant sludge. Kos (1976) in addition suggests that the solids concentration not only was a function of the compressive stress but also of the varying flow conditions. What is needed now are appraisals of the various models to determine their applicability to plant-size thickeners.

CHAPTER 3

STUDY OBJECTIVES

In view of some of the problems noted in the literature review, and the practical importance of these problems, it was thought useful to make an experimental study of the effects of certain parameters on thickening.

The objective of the study was to examine the effect of two independent variables on the dependent variables using a factorial design. The independent variables to be studied were flocculant dosage and solids throughput. The levels of the independent variables chosen were based on plant-size thickening operations. The dependent variables examined were concentration of underflow solids, underflow withdrawal rate, overflow rate, overflow quality, and steady state solids concentration profile.

The data obtained were to be used to show the importance of the flocculant dose in the thickening of compressible slurries.

CHAPTER 4

EXPERIMENTAL APPROACH

To satisfy the objectives yet keep the scope within the time and resources available, it was important to select the variables carefully. This led to an experimental design which kept the number of experiments to a minimum. This section discusses the variables in the experimental study, the equipment that was utilized to measure and control the variables, and then traces the procedure used.

4.1 Variables

To restrict this scope, the following potential variables were fixed: temperature, column diameter, height of mud bed, pH, concentration of solids (within experimental limits), sampling points, place of polymer addition, mixing procedures and type of polymer.

The independent variables included the solids throughput, inlet concentration (with some uncontrolled variability), mud bed height and flocculant dose and type. Since the known large scale "deep thickeners" operate with a mud bed height of 9 m or higher, the bed height was maintained constant around 9 m for this current pilot scale project. A "deep thickener" is a form of thickener in which an attempt is made to increase the underflow solids concentration

by operating with an unusually deep bed of solids in compression to provide a "dewatering pressure" on the lowest layers of the suspension.

The feed percent solids was maintained at about 12% by a wash to slurry volumetric ratio of 1.5:1. This was chosen to obtain a "reduced" net wash of approximately 2 which is the usual result from the plant processing bauxite A. The "reduced" net wash is the mass of wash water introduced less the mass of water travelling with the underflow, all per unit mass of solid phase. The variability of the inlet solids concentration made analyses of results a challenge.

The solids throughput was varied over the range analogous to that used on an existing large scale "deep thickener" processing mud from bauxite B. The solids flux, kg. h^{-1}. m^{-2}, was used as the scale down parameter with values of 100 to 200 kg. $h^{-1}.m^{-2}$. For the current pilot plant unit, the resultant solids throughput was approximately 0.8 to 1.5 kg. h^{-1}. So these limits were the elected levels for the solids throughput.

The synthetic flocculant chosen for this study was Cyanamid product RMD-30, an anionic polymer having a nominal mean molecular weight of 6 to 8 x 10^6 and a 95% degree of hydrolysis. The levels of dosage selected were 0.05 and 0.10 kg RMD-30/2000 kg dry mud.

An interaction is possible between the flocculant dose and the wash to slurry ratio (i.e. solids concentration of feed). So for each run, the feed solids concentration was kept constant, within experimental accuracy, at 12%.

The dependent variables measured were:

(a) Underflow solids concentration,

(b) Rate of withdrawal - this depended on maintaining bed height constant (indirectly related to solids throughput and compression rate),

(c) Steady state solids concentration profile throughout column,

(d) Overflow rate, and,

(e) Overflow quality.

4.2 Experimental Design

The experimental design was a two level, two variable factorial one. Table 4-1 relates the variable levels to their codes and Table 4-2 shows the design matrix. Although the runs described in these tables were performed with mud from bauxite A, a run was also performed with bauxite B (using solids flux and flocculant dosage encountered in plant processing bauxite B).

TABLE 4-1. Variables and their Coded Levels

Variables	Uncoded Level	Coded Level
Solids throughput ($kg.\ h^{-1}$)	1.0 1.5	-1 +1
Flocculant dose $\frac{kg\ RMD\text{-}30}{2000\ kg\ dry\ mud}$	0.05 0.10	-1 +1

TABLE 4-2. Design Matrix

Solids throughput	Flocculant dose
-	-
+	-
-	+
+	+

4.3 Apparatus

The apparatus consisted of a feed assembly, a plexiglass column shown in Fig. 4-1, and a discharge collection area.

In the feed section, the mud slurry and wash water were held in reservoirs each with a maximum capacity of 190 litres (42 gallons). The mud slurry was maintained at room temperature as it was stored in the environs of the feed section. It was kept uniformly dispersed by a 1/4 H.P., 1725 RPM Master Gearmotors mixer. The set speed for this mixer was a compromise between that which would permit sand to settle out and that which would entrap a noticeable quantity of air. The distilled water was also at room temperature as it was collected and placed in the feed area the day before a run in order to attain equilibrium with the room temperature. A 1/4 H.P., 100/1800 RPM Lightning mixer was employed to keep the synthetic flocculant well dispersed in the distilled water. The distilled water drum carries a level indicator which provided another way of checking the wash water flow rate by the volume-time method. A level indicator was not installed on the mud slurry drum as no meaningful measurements could have been obtained due to the presence of the high turbulence within the drum.

The column was fed with mud slurry and wash water by means of calibrated console Masterflex pumps, each capable of supplying a volumetric flow rate of 0.2 to 378 cm^3/min. The desired flow rates were set on these pumps, and they were checked periodically during a run by the volume-time method. The wash water and slurry met at a T-joint where mixing took place. This slurry-water mixture was conveyed to the feed well by a single tubing length. The temperature of the

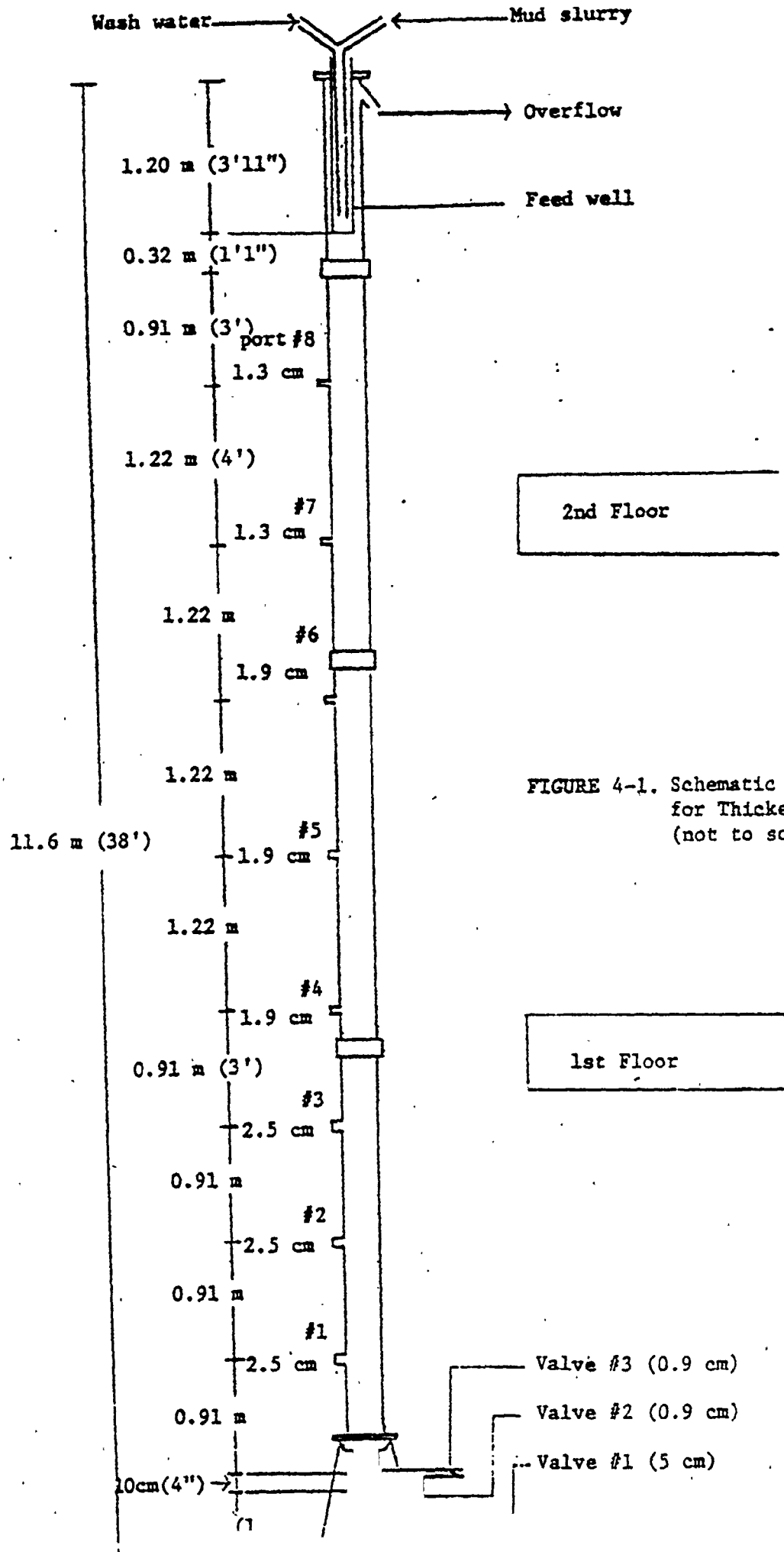

FIGURE 4-1. Schematic of Column Used for Thickening Tests (not to scale)

materials in the feed section was ascertained during operation from samples collected at set time intervals for the following analyses given in Table 4-3.

TABLE 4-3. Analyses Done on the Streams

	Feed Mud Slurry	Overflow	Underflow
Total Titratable Soda	✓	✓	✓
Alumina Concentration	✓	✓	✓
Caustic Concentration	✓	✓	✓
Solids Concentration	✓	✓	✓
Liquid Density	✓	✓	✓
pH	✓		✓
Residual Flocculant		✓	

The column, which was 10.2 cm (4 inches) in diameter and 11.1 m (36.4 feet) high, had a feed well of diameter 1.9 cm and length 1.2 m. Sample ports were located throughout the length of the column. The positions and sizes of the ball valves at each port are shown in Figure 4-1. Slurry samples (≈500 mL volume) were obtained from each

sample tap at steady state (ascertained by the solids content of the underflow as a function of time). The sampling was done from the highest to the lowest point within ten minutes. For the sample aliquots, the solids concentration and particle size analyses were obtained quantitatively. The discharge collection area had reservoirs for storage of overflow and underflow. The overflow from the column was conveyed by a length of hose to a 190 litre (42 gallon) drum. By means of a level indicator at the side, the average overflow rate for a run was determined by the volume-time method. This was very important as this flowrate could be obtained more accurately this way than by checking it while liquid was being discharged and making allowances for the periods of time when no overflow was obtained. The analyses performed on the overflow are indicated in Table 4-3.

There were three outlets for the underflow discharge as illustrated in Figure 4-1, each outlet size being 0.9 cm (3/8 inch) in diameter. During the course of experimentation, outlets 1 and 2 were used separately as discharge routes. The discharge was connected to a Moyno pump driven by a motor (225 RPM). An automatic timing device (assembled in the workshops of the Research Centre) switches on the pump for a certain time interval at a set time (every 15 or 30 minutes). In order to see whether the apparatus was operating under steady state conditions, the density of the underflow discharge was determined periodically by a volume-weight method. Underflow samples were collected throughout operation of the column for the analyses indicated in Table 4-3. The underflow rate of the experimental thickener was calculated by a mass balance and also by the volume of underflow amassed over the run period.

4.4 Materials

The materials used in the deep thickening tests are red mud slurries, distilled water, synthetic flocculant and tracers.

Red muds are insoluble residues left from the alkaline extraction of alumina from bauxite. The mud slurry obtained from the plant processing bauxite A had a variable chemical composition and particle size analysis which were functions of plant conditions and the quality of raw materials employed. In order to minimize errors due to this variation, more than enough slurry was collected in order to execute four runs. The mud slurry was screened (-50 mesh) to remove large scale particles then it was characterized by quantitative and qualitative analyses, (See Appendix B). Apart from possible alumina hydrate precipitation, no other major effect of aging the mud slurry over a few months is known.

As a wash for the mud slurry, distilled deionized water was used due to the variable nature of tap water during the spring thaw and also because of the unknown effect of water impurities on the synthetic flocculant.

An anionic polymer, RMD-30, with a nominal mean molecular weight of 6 to 8 x 10^6 and a 95% degree of hydrolysis was the synthetic flocculant selected. It was prepared in stock solutions of 0.25 g RMD-30/L. For each test, a calculated quantity of RMD-30 stock solution (to give the required flocculant dose) was added to a known volume of distilled water.

Throughout the four experimental runs, three different materials were appropriated for use as tracers, namely, zinc sulphide, alumina and calcium sulphate. The criteria for selection of the tracer were its density in relation to mud particles, insolubility in the caustic solution and its ability to be easily seen in the mud bed.

4.5 Experimental Procedure

A 0.025% stock solution of RMD-30 was made up within one day of an experimental run. Details of the stock solution preparation are given in Appendix A.1. The appropriate quantity of stock RMD-30 solution was added to the drum of distilled water depending on the desired dry mud throughput, flocculant dose and wash water flowrate. Sample calculations are shown in Appendix D. In order to disperse the RMD-30 polymer well, the flocculant-water solution was mixed for 1.5 hours before use.

Meanwhile, the tracer was prepared by screening then collecting a known weight below a certain size. The purpose of the tracer was to provide an idea of the residence time of the mud particles in the column. This was obtained by noting the time interval between addition of the tracer and its exit with the underflow.

Meanwhile, the wash water and mud slurry flow rate (to give the desired solids throughput) were set on the Masterflex pump scales (corresponding to pump heads in use). The column was then fed with mud slurry and wash water at these rates. When the required mud bed height was attained, the tracer was added through the mud slurry line (while simultaneously cutting off the mud slurry feed) in a manner to simulate a pulse. Although the column was not operating under steady state conditions at the time of addition, time constraints set on the tests forced the addition then.

After the tracer addition, the automatic timing device regulating the underflow was turned on. The period of underflowing was

adjusted (during the thickening test) so that the mud bed height could be controlled within certain limits (± .10 m). Steady state column operation was determined by the underflow density which was monitored regularly.

The length (24 - 32 hrs) of operation of the experimental thickener was such that it was functional for a few hours after the discharge (or supposed one) of the tracer. Samples and measurements were taken throughout the operational period at several intervals. This schedule is illustrated in Table 4-4.

4.6 Analytical Methods

The analytical methods used for the tests indicated in Table 4.3 and the red mud characterisation are tabulated in Table E-2. The exact details of these methods are proprietary.

Concerning the measurement of residual flocculant, there is no very good analytical procedure available for very small quantities of synthetic flocculants in Bayer liquors containing other organics in solution. In this work, an indirect empirical test was used whereby the filtration rate of a sample under given conditions was sensitive to the concentration of synthetic flocculant. The concentration of RMD-30 in the overflow liquor was obtained by comparing the filtration times with those of known concentrations of RMD-30 in a similar liquor. This method is outlined in Appendix A-2.

TABLE 4-4. Sampling Schedule

Time Intervals in Hours					Hours After Start-Up			
Run #	I	II	III	IV	I	II	III	IV
Feed	2	2	4	5	0	14	0	0
Overflow	2	2	2	2	16	14	24	19
Underflow	1	1	2/1	2/1	0	0	0/24	0/20
Sample port #8	0	4	6	4	end of test	16	24	20
Sample ports #'s 1 to 7	0	0	0	0	end of test	end of test	end of test	end of test

Time Intervals from Start-Up (hr)

Run Number	I	II	III	IV
Mud bed height	0.5	0.5	0.5	0.5
Temperature	as samples collected			
Slurry flow rate	2	2	3	2
Water flow rate	2	2	3	2
Volume of wash water remaining	2	2	2	2
Volume of overflow collected	3	2	3	2
Overflow rate	2	2	2	2
Volume of underflow collected	batchwise measurement			

CHAPTER 5

RESULTS

This section presents a concise summary of the results obtained from the continuous runs and the batch settling tests.

Figures 5-1 and 5-2 show the concentration of solids in the bed as a function of bed height for the different conditions. In figure 5-1, the data for Run III show the concentration to be relatively independent of depth except near the bottom where the solids concentration increases markedly. For Runs I and II, the column was misaligned at height 3.35 m (11 ft) and the data show an oscillating variation in concentration with depth. All solids concentration profiles, except that of Run IV, show a noticeable increase of solids concentration with depth near the bottom. Table 5-5 gives the numerical results of the solids concentration profile which are portrayed graphically in Figures 5-1 and 5-2. The steady state solids concentration profiles are shown as a function of the bed height and the time of operation.

A summary of the experimental conditions and results is presented in Table 5-1. Run IV was performed with mud from bauxite B which required a higher flocculant dose than mud from bauxite A. The residence time of an average mud particle in the column was measured by the stimulus-response technique, which showed that the residence time increased with a decrease in solids throughput. Concerning tests performed with mud

from bauxite A; a negligible increase in the real separation efficiency (η_{REAL}) and a decrease in the pseudo separation efficiency (η_{PSEUDO}) was noted when the solids throughput decreased. Refer to Appendix E-2 for definitions of these separation efficiencies.

Table 5-2 shows the mass flow rates and solids concentration of the streams entering and leaving the column. The slurry feed and wash water flow rates of Runs I and II are approximately equal, the difference being a higher flocculant dose applied during Run II. At steady state the solids content of the underflow of Run II was greater than that of Run I. During Run III, although a lower slurry feed mass flow rate was employed than in Run II, a lower underflow solids content was obtained. The results of Table 5-2 were used to calculate the separation efficiencies.

The mixing efficiency of each experimental run is presented in Table 5-3. The concentration of the total titratable soda in the feed overflow and underflow streams were used to determine the mixing efficiency. This gives an idea of the mixing efficiency of the synthetic flocculant. The mixing efficiency of Run IV is much lower than the other Runs; for this run, the concentration driving force is lower.

Table 5-4 shows the adsorption efficiencies of the polymeric flocculant employed, RMD-30, a product of Cyanamid. This was calculated by a filtration method (refer to Appendix A.2) which indicated a lower adsorption efficiency in Run II than in Run I.

Figure 5-3 displays the mud bed height as a function of time for Runs I to III at zero solids throughput. Table 5-6 shows the rate of the mud bed fall as a function of the weight of dry solids in the bed. These were determined from Figure 5-3 by obtaining the gradients at the appropriate points. From Table 5-6 it is seen that the higher the weight

of dry solids in the bed, the lower the rate of fall of the bed. But after 2.5 days, the rate of decrease of the bed depth was approximately the same for Runs II and III which had similar flocculant doses. Run I, wherein a lower flocculant dose was employed, had a lower rate of bed depth decrease after 2.5 days.

The results of the batch settling tests performed on mud from bauxite A are shown in Table 5-7. The variables in the settling tests were the initial solids concentration and the flocculant dose. These results demonstrated that an increase in flocculant dose increased the initial settling rate. But the higher the initial solids concentration employed, the lower the initial settling rate for the same flocculant dose. The calculated compression point increases with increase in initial solids concentration. But due to the subjective judgement involved in arriving at these results, the limits of accuracy ranged from ± 1% (for a flocculant dose of 0.05 kg RMD-30/2000 kg dry mud) to ± 2% (for a flocculant dose of 0.10 kg RMD-30/2000 kg dry mud). For the batch settling test with an initial solids concentration of 24% and the lower flocculant dose, the limits of accuracy could not be determined because the test was not continued long enough.

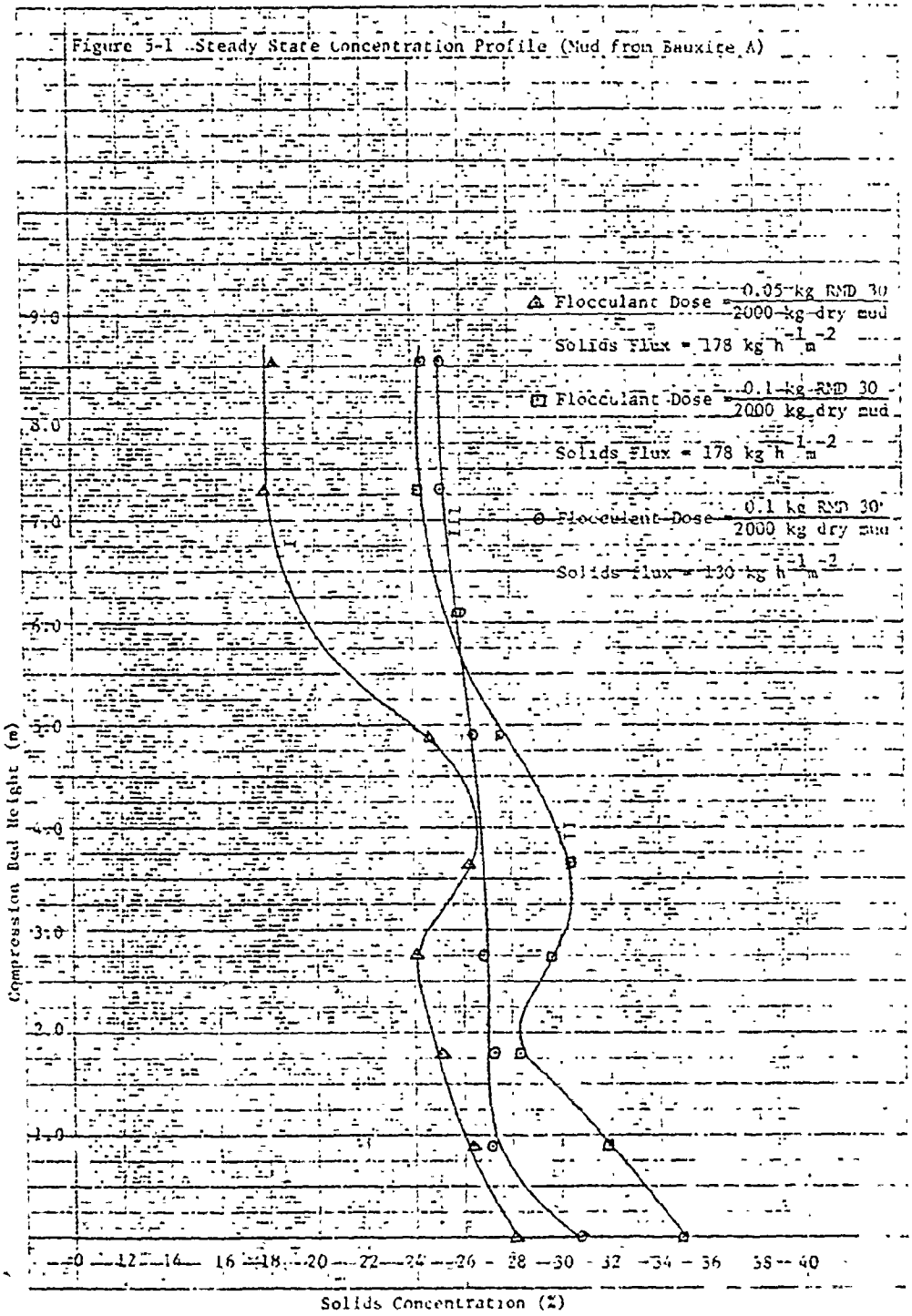
Figure 5-1 Steady State Concentration Profile (Mud from Bauxite A)
Flocculant Dose = 0.05 kg RMD 30 / 2000 kg dry mud
Solids Flux = 178 kg h⁻¹ m⁻²
Flocculant Dose = 0.1 kg RMD 30 / 2000 kg dry mud
Solids Flux = 178 kg h⁻¹ m⁻²
Flocculant Dose = 0.1 kg RMD 30 / 2000 kg dry mud
Solids Flux = 130 kg h⁻¹ m⁻²
Compression Bed Height (m)
9.0
8.0
7.0
6.0
5.0
4.0
3.0
2.0
1.0
0 12 14 16 18 20 22 24 26 28 30 32 34 36 38 40
Solids Concentration (%)

FIGURE 5-2. Steady State Concentration Profile - Mud Processed From Bauxite B

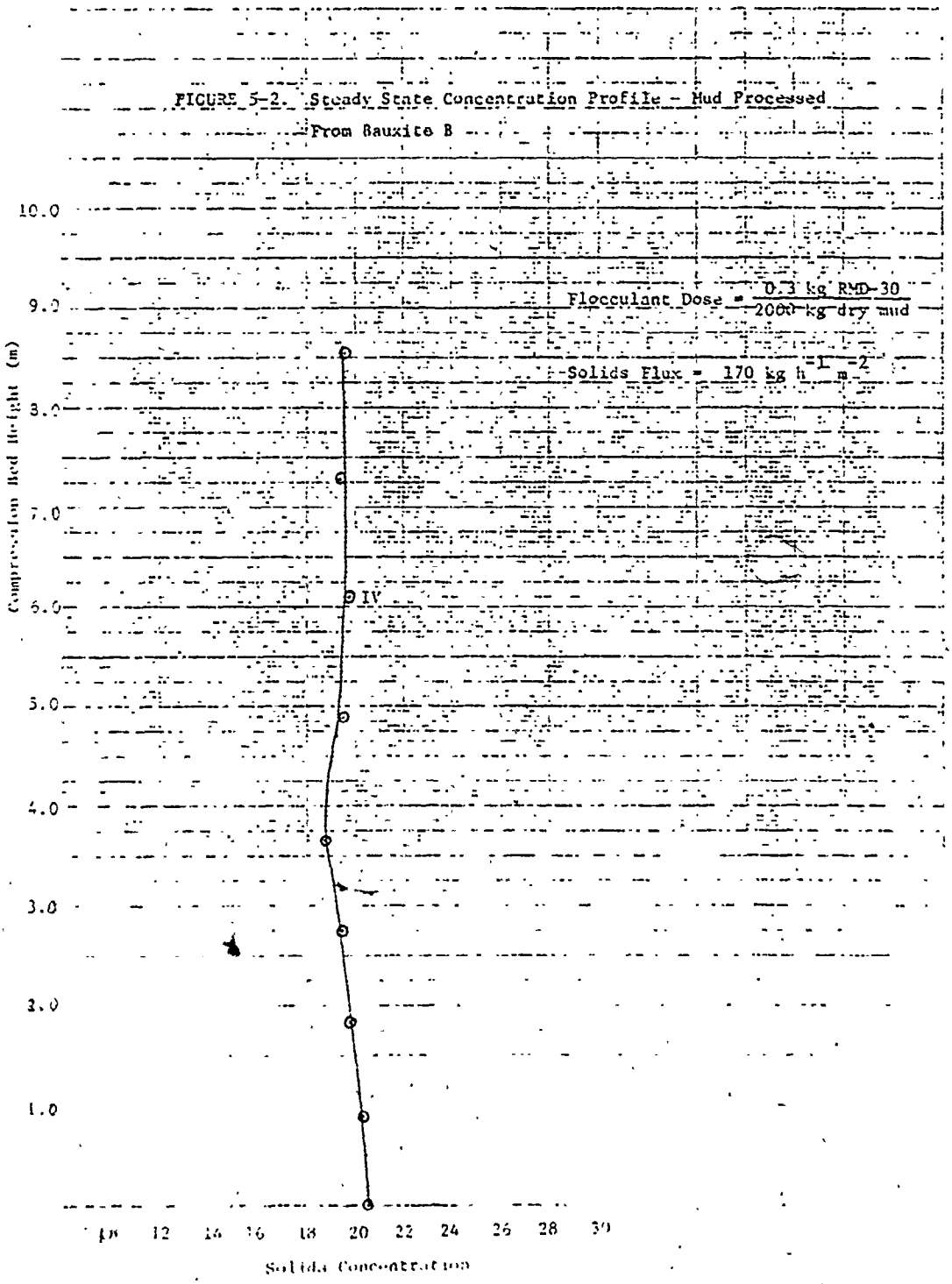

TABLE 5-1. Summary of Experimental Conditions and Results

Run Number	Flocculant Dose kg RMD-30 / 2×10^3 kg dry mud	Slurry Flow Rate cm^3/min Set / Average $^{\#2}$+	Solids Throughput kg/h Set / Average*	Wash Water Flow Rate cm^3/min. Calculated / Measured $^{\#1}$	Solids Flux $kg/h.m^2$ Set / Average*	Average Overflow Rate+ $cm^3/min.$	Net Bed Height Increase Rate+ cm/min.	Average Underflow Rate $cm^3/min.$	Underflow Pump Rate $cm^3/min.$	Tracer	Approx. Residence Time hr	η_{REAL} %	η_{PSEUDO} %
I	0.05	70 / 70	1.44 / ±.04 1.46	105 / 100	178 / 180	90	1.0	75* / 71+	1400[2]	Zn S[A]	16-17	59	1
II	0.10	70 / 66	1.44 / ±.04 1.42	105 / 100	178 / 175	112	0.9	52* / 61+	350[1]	Alumina[B]	could not observe	66	19
III	0.10	50 / 52	1.08 / ±.04 1.12	75 / 69	133 / 117	75	0.65	48* / 48+	350[1]	Calcium Sulphate[C]	23	67	6
IV	0.30	115 / 108	1.47 / ±.03 1.38	45 / 45	182 / 170	45	0.7	98* / 89+	350[1]	Calcium Sulphate[D]	not observed	30	9

\+ measured
* calculated
2 - underflow outlet #2
1 - underflow outlet #1

A prepared by slurrying with mud 100 g of -325 mesh fraction
B prepared by slurrying with mud 100 g of -200 mesh fraction
C prepared by slurrying with overflow liquor 200 g of -20 mesh fraction
D prepared by slurrying with overflow liquor 150 g of -30 mesh fraction

TABLE 5-2. Mass Flow Rates and Solids Content of Streams of Experimental Runs

Run Number	Mass Fraction Solid in Slurry Feed, s_1**	Slurry Feed Mass Flow Rate, S_1* g/min	Wash Water Mass Flow Rate, L_1*, g/min	Mass Fraction of Solid in Diluted Feed, w_1	Diluted Feed Mass Flow Rate, W_1+ g/min	Overflow Solids Concentration** mg/L	Overflow Mass Flow Rate, W_2* g/min	Mass Fraction Solid In Underflow w_3**	Underflow Mass Flow Rate, W_3 g/min
I	0.277	88	100	0.125+	188	100	91	0.280	89+ 88*
II	0.285	83	100	0.127+	183	104	113	0.348	69+ 80*
III	0.286	65	70	0.123**	135	154	76	0.305	61+ 61*
IV	0.184	125	44	0.136**	169	59	45	0.200	115+ 104*

\+ Calculated by mass balance

* Calculated from Volumetric flow rate measurements

** Measured

TABLE 5-3. Mixing Efficiencies of Experimental Runs

Run Number	Average Feed T.T.S. Concentration g/L	Mass Fraction Soluble Component in Feed $x_{u,n-1} \times 10^3$	Average Steady State Overflow T.T.S. Concentration g/L	Mass Fraction Soluble Component in Overflow $X_{o,n} \times 10^3$	Average Steady State Underflow T.T.S. g/L	Mass Fraction Soluble Component in Underflow $x_{u,n} \times 10^3$	Mixing Efficiency $E_n = \frac{x_{u,n-1} - x_{u,n}}{x_{u,n-1} - X_{o,n}} \times 100$
I	24.0	23.3	9.0	8.9	9.7	9.6	95
II	24.3	23.6	8.9	8.8	10.9	10.8	86
III	24.0	23.3	9.8	9.7	10.9	10.8	92
IV	13.3	12.9	7.2	7.1	10.4	10.3	45

T.T.S. ≡ Total Titratable Soda

TABLE 5-4. Adsorption Efficiencies of Polymeric Flocculant RMD-30

Run Number	Initial Flocculant Concentration in Diluted Slurry, F_I mg/L liquor	Average Filtration Time of Overflow SEC	Residual Flocculant Concentration, F_R mg/L	Adsorption Efficiency $E_F = \frac{F_I - F_R}{F_I} \times 100$
I	3.5	1.4	0	100
II	7.3	2.7	0.4	94

TABLE 5-5. Steady State Solids Concentration Profiles of Experimental Runs

			Solids Concentration (%) at a Given Location From Bottom of Column								
Time Column Operating hr	Bed Height m	Location from Bottom m / Run Number	0.0 Underflow	0.91	1.83	2.74	3.66	4.88	6.10	7.31	8.55
23	9.24	I	28.0	26.3	25.0	24.0	26.2	24.6	28.7	17.9	18.3
20.5	9.16	II	34.8	31.8	28.3	29.6	30.4	27.5	25.8	24.2	24.4
32	9.2	III	30.7	27.1	27.2	26.8	26.3	26.4	25.9	25.1	25.1
26	9.15	IV	20.4	20.2	19.6	19.4	18.7	19.5	19.7	19.4	19.5

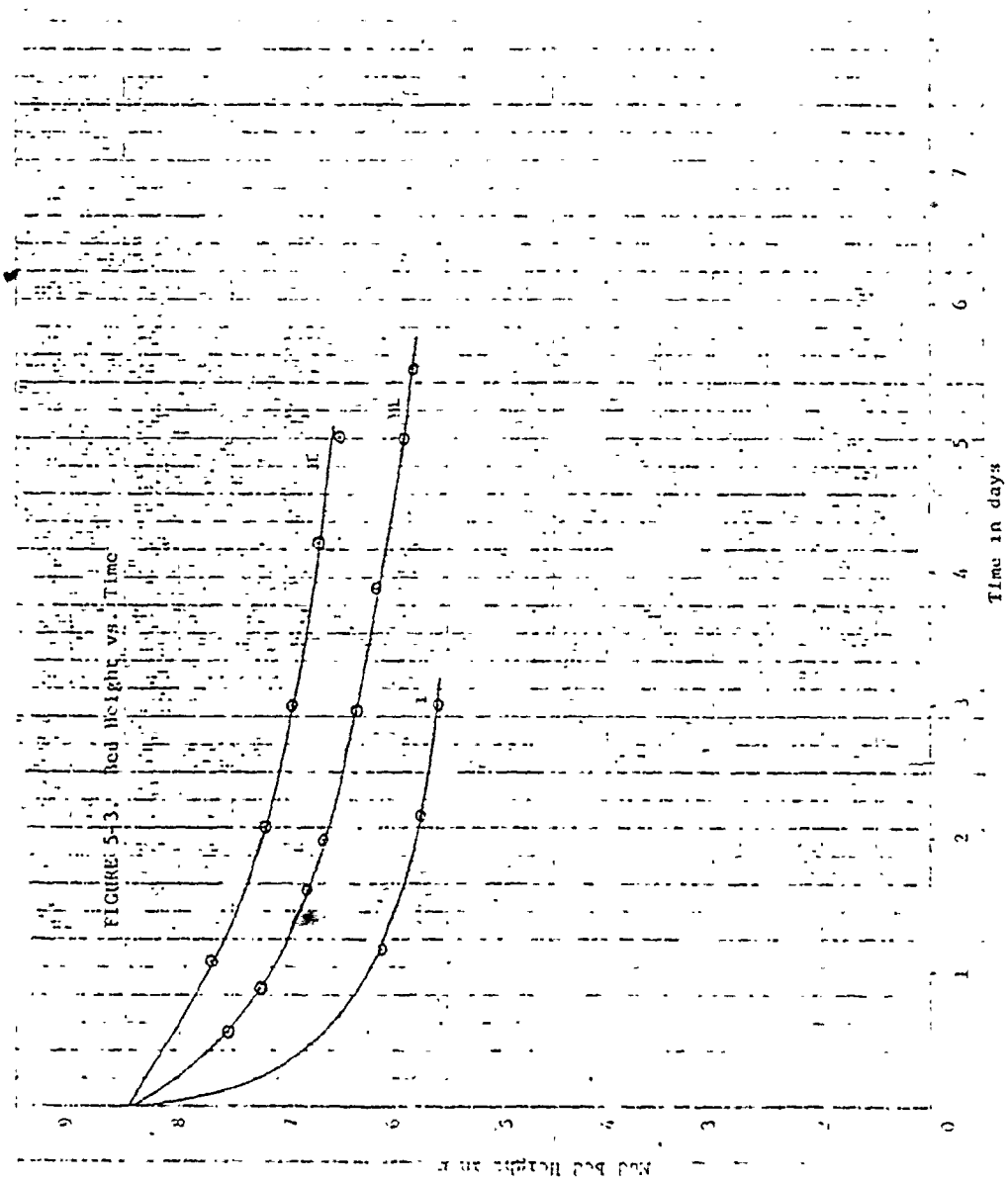

FIGURE 5-3. Bed Height vs. Time

TABLE 5-6. Rate of Bed Decrease as a Function of Dry Solids Weight in Bed

Run Number	Flocculant Dose $\frac{\text{kg RMD-30}}{\text{2000 kg dry mud}}$	Steady State Weight of Dry Mud in Bed + kg	Initial Rate of Slurry-Supernatant Interface Fall* m/hr	Rate of Fall After 2.5 Days cm/hr
I	0.05	20.4	0.36	0.64
II	0.10	25.4	0.03	1.08
III	0.10	23.8	0.11	1.05

* After removal of samples for concentration profile determination

\+ Obtained by graphical integration

TABLE 5-7. Results of Batch Settling Tests Performed on Mud from Bauxite A as a Function of Initial Solids Concentration and Flocculant Dose

Dilution of 40% Solids Slurry	Initial Solids Concentration %	Flocculant Dose g RMD-30 / 2000 g dry mud	Initial Settling Rate cm/hr	Compression Point (Method of Panov and Kuznetsov (1973)) Solids Concentration	
				g/cm^3	%
1/10	6	.05	208	.14	13(±1)
		.10	1224	.22	19(±2)
1/5	11	.05	20	.22	19(±1)
		.10	51	.23	20(±2)
1/4	14	.05	12	.25	22(±1)
		.10	35	.24	21(±2)
1/2	24	.05	4	.30	25
		.10	20	.29	24(+1)

CHAPTER 6

DISCUSSIONS

This chapter is divided into two parts, the first concerns the observed behaviour of the mud in the column and the second part examines the effects of various factors on the thickening characteristics of the mud.

6.1 Observations of Mud Flow Behaviour

The characteristics of flow of the solid and liquid portion of the slurry was observed and these are described in this section.

6.1.1 Solid Flow Characteristics

All the tracers used (except for alumina which was not observed) moved through the column in a fashion analogous to a plug. This solids flow behaviour is not similar to that observed by Chandler (1976) for a full-scale thickener. Therefore, the thickening characteristics of mud obtained from this column may not simulate that of a full-scale thickener.

6.1.2 Liquid Flow Characteristics

The phenomenon of channelling was observed when experimenting with mud from bauxite B which was manufactured in the pilot-plant. Small diameter, crooked channels were seen at a height of 2.4 m and

higher. But although channelling was not seen in the section below 2.4 m and with tests using mud from bauxite A, this does not exclude the existence of channelling for these cases. Also, with mud from bauxite B, mound formations were observed at the slurry-supernatant interface. These formations resembled volcanoes erupting at the surface (Figure 6-1).

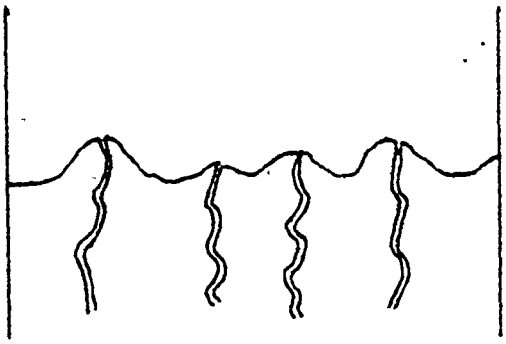

FIGURE 6-1. Schematic Representation of Mound Formations

The occurrence of channelling which augments liquid drainage rates has been observed by countless researchers who include Coe and Clevenger (1916), Dell and Sinha (1966), Scott (1968a), Chakravarti and Dell (1969), Harris et al (1975) and Kos (1977). Coe and Clevenger (1916) observed volcano formation at the slurry-supernatant interface as well as Roberts (1934) who reported seeing channelling and mound formation at the interface. The mound formation was explained as being due to liquid in channels breaking the surface. Both mound formation and channelling was observed with mud processed from bauxite B.

6.2 Effect of Various Factors on the Thickening of Red Mud

This section discusses the effect of different factors on the thickening of red mud. First of all, the effect of the operating variables, namely, the solids throughput and synthetic flocculant dose is dealt with. Next, the combined effect of the diameter to length ratio and operational temperature is examined. Then, the interface subsidence rate as a function of the dry solids weight in the bed is discussed. Finally, the effect of the flocculant dose and solids concentration on the compression point (determined from batch settling tests) is reviewed.

6.2.1 Effect of Solids Throughput

The effect of solids throughput on the residence time of the solid particles and the separation efficiency is examined in this section.

6.2.1-1 Effect of Solids Throughput on the Residence Time

The effect on residence time is shown in Table 6-1. It was noted that a 23% decrease in solids throughput resulted in the average mud particle residing for a 44% longer time period in the column. This finding is consistent with theory because with a reduction in solids throughput (bed volume unchanged), the residence time increases as predicted by the following relationship,

$$\tau = \frac{V}{v} (1 - \phi) \qquad \text{eqn. 6-1.}$$

TABLE 6-1. Effect of Solids Throughput on Residence Time of Mud

Run	Solids Throughput kg/hr	% Change	Residence Time hr	% Change	Mixing Efficiency En	No. of Percentage Units Change	Flocculant Dose kg RMD-30 / 2000 kg dry mud	% Change	η_{REAL} %	No. of Percentage Units Change	η_{PSEUDO} %	No. of Percentage Units Change
I	1.46	-23	16-17	+44	95	-3	0.05	+50	59	+8	1	+5
III	1.12		23		92		0.10		67		6	

TABLE 6-2. Effect of Solids Throughput on Separation Efficiency

Flocculant Dose = 0.10 kg RMD-30/2000 kg dry mud

Run	Solids Throughput kg/hr	% Change	η_{REAL} %	No. of Percentage Units Change	η_{PSEUDO} %	No. of Percentage Units Change	Mixing Efficiency, En, %	No. of Percentage Units Change
II	1.42	-21	66	+1	19	-13	86	+6
III	1.12		67		6		92	

where τ = residence time

V = bed volume

v = throughput (volume/unit time)

$= v_s/P_s$

v_s = solids throughput

P_s = solids density

ϕ = porosity

which predicts a 50% increase in residence time when the solids throughput is decreased by 23%. But the relationship given is not as simple for a consolidating bed of sludge because the porosity increases with increasing height.

Comings et al (1954) ran thickening experiments with the same bed height and various feed flow rates to give different detention times. But the detention times were calculated values and there was insufficient information to estimate the solids throughput; so a comparison with the author's result was not possible. A literature search was fruitless in obtaining results of the effect of the solids throughput on measured residence times.

6.2.1-2 Effect of Solids Throughput on the Separation Efficiency

This effect, shown in Table 6-2 demonstrates that a 21% decrease in solids throughput (maintaining flocculant dosage and inlet concentration constant) gave rise to a negligible change in the real separation efficiency, η_{REAL}, and a 13% reduction in the

pseudo separation efficiency, η_{PSEUDO}. Definitions of these efficiencies are given in Appendix E-2. But, one would expect an increase or a negligible change in both η_{REAL} and η_{PSEUDO} when the solids residence time is increased.

From steady state thickening results, Kos (1977) using water treatment sludge obtained a 7% increase in underflow concentration when the solids throughput was decreased by 36% (bed height constant). With a deeper bed, a 64% decrease in the solids throughput resulted in a 30% increase in the underflow sludge concentration. The possible reasons for this anomalous effect of solids throughput on efficiency noted by the author are outlined below:

(a) Column Misalignment

The results, shown in Figure 5-1, from Runs I and II suggest that the column was improperly aligned. This fault was corrected before Run III was performed. As a sidenote, the rapid increase of solids concentration with depth in the vicinity of the crooked column or one which incorporates baffles would improve the separation efficiency, and possibly in a shorter depth than 9 m.

(b) Sampling Procedures

During Run II, a mud sample was extracted by means of underflow valve No. 2 three hours before the test was completed. This sample had a solids content 5% higher than the underflow at that time. The mud is thicker due to the longer than average residence time (approximately zero velocity at the wall) and also because of a build-up of mud around the outlet (illustrated in Figure 6-2) in the form of a cone outline.

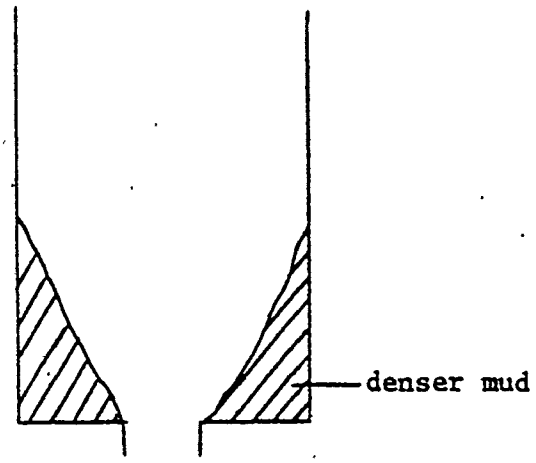

FIGURE 6-2. Diagram Illustrating Cone-Shaped Mud Build-Up

Evidence of this thicker mud was shown by the steady state concentration profiles (Figure 5-1). The greatest increase of solids concentration with depth is in the region just above the underflow outlet. A steep increase of solids concentration with depth was also noted in the vicinity of the misaligned joint for Runs I and II. From an observation of compression zone concentration profiles, the following investigators listed in Table 6-3 also obtained the steepest solids concentration gradient in the region just above the underflow outlet.

TABLE 6-3. D/L Ratios of Columns Used by Investigators Who Obtained a Marked Dependence of Solids Concentration with Depth Near Bottom of Column

Investigator	Column D/L Ratio x 10^3	Slurry Type
Comings et al (1954)	159	Ca CO_3, clay
Smiles (1976)*	273	red mud
Kos (1977)	125	water treatment plant
* Centrifuge tube used		

Smiles (1976) attributed this result to sorting whereby the sand tends to accumulate at the bottom, thereby enhancing the concentration gradient. After he removed the sand portion and repeated the experiment, this steep increase disappeared. The concentration gradients obtained by Stinson (1979) did not show this phenomenon. The materials used were Australian red mud (50% sand) and Jamaican red mud (8% sand), where sand is defined as particles greater than 150 μm in size. Because the portion of red mud particles greater than 150 μm in size were screened out for Stinson's experiments, the absence of the steep concentration gradient supports Smiles' (1976) claim that the gradient is due to sorting.

For the experiments being discussed, sorting could be a reason for this phenomenon as particles larger than 297 μm in size were removed from the mud. But mud from bauxite B did not show this significant increase of solids concentration with height near the outlet (see Table 6-4). This suggests that for each mud type in combination with a given D/L ratio, there is a throughput value above which this phenomenon is not observed. The sampling of valve No. 2 may have disturbed ~~this~~ thicker mud, which on mixing with the thinner mud near the centre of the column augmented the underflow solids concentration, thereby resulting in a higher than would be expected (comparing Run III) η_{REAL} and η_{PSEUDO}.

Probably this sampling, in combination with the misaligned column, affected the separation efficiency significantly. These findings suggest that a thickener with two or more outlet openings (one at the bottom and the other(s) in the sides in the vicinity of the mud cone) which are alternately used will improve the separation efficiency.

TABLE 6-4. Steady State Overall and Bottom 0.9m Depth Concentration Gradient

Run	Throughput kg/h	Flocculant Dose kg RMD-30 / 2000 kg dry mud	Overall Solids Concentration Gradient % Solids / m	Percentage Increase	Bottom 0.9m Depth Concentration Gradient % Solids / m	Percentage Increase
I	1.44	0.05	$\frac{28 - 18.3}{8.55} = 1.13$	8	$\frac{28 - 24.3}{0.91} = 1.87$	143
II	1.44	0.10	$\frac{34.8 - 24.4}{8.55} = 1.22$	-47	$\frac{34.8 - 31.8}{0.91} = 3.30$	66
III	1.08	0.10	$\frac{30.7 - 25.1}{8.55} = 0.65$		$\frac{30.7 - 27.1}{0.91} = 3.96$	
IV	1.47	0.30	$\frac{20.4 - 19.5}{8.55} = 0.10$		$\frac{20.4 - 20.2}{0.91} = 0.22$	

(c) Flocculant Dosage Rates

A minor difference in the applied flocculant dosages between Runs II and III might account for the observed irregularity. Calculations of the flocculant doses from the experimental results are given in Table 6-5. Although the dosage for Runs II and III

TABLE 6-5

Flocculant Doses Estimated From Observations	
Test	Flocculant Dose $\frac{\text{kg RMD-30}}{\text{2000 kg dry mud}}$
I	0.05 ± 0.003
II	0.105 ± 0.003
III	0.094 ± 0.003

are statistically different, that is, the maximum possible value from Run III is less than the minimum possible value from Run II, nevertheless, the overall effect on the results should be small. Also, the mixing efficiency of the streams in Test III is 6% higher than those of Run II; therefore, this increase may have resulted in a higher separation efficiency which would have nullified the effect of the dosage difference.

(d) Optimum Conditions

There may be an optimum solids throughput to achieve the greatest separation efficiency. But this is unlikely as after each test when there was no inflow or outflow, the bed height kept on decreasing with time. This showed that the underflow solids concentration increased (and therefore also the separation efficiency) with time.

In consideration of the above discussion, it appears as if the separation effiency, η_{PSEUDO}, calculated for Run II is higher than expected due to the column misalignment and disruption of the mud cone. Therefore, this has to be taken into consideration when comparing the results of Runs I and II with those of the other Runs.

6.2.2 Effect of Flocculant Dose on the Separation Effiency

For the current data, Table 6-6, a 50% increase in the RMD-30 dose resulted in a 7% larger real separation efficiency, η_{REAL}, and an 18% increase in the pseudo separation efficiency, η_{PSEUDO}. The η_{PSEUDO} increase seems unexpectedly large in comparison with other data (see subsection 6.1.2). Nevertheless, the effect of an increase in dosage appears to be favourable to the separation efficiency.

The larger dose should improve the separation efficiency due to the formation of a more extended particle-flocculant network which makes the sediment more sensitive to pressure from above. The more extended network is as a result of the adsorption of a greater quantity of RMD-30 per unit area of mud particles. The adsorption efficiency of the polymeric flocculant diminished by 6% (Table 6.6) which would

TABLE 6-6. Effect of Flocculant Dose on the Separation Efficiency

Solids Throughput = 1.44 kg/h									
Run	Flocculant Dose, kg RMD-30 / 2000 kg dry mud	η Real, %	Number of Percentage Units Change	η Pseudo, %	Number of Percentage Units Change	Mixing Efficiency E_n, %	Number of Percentage Units Change	Flocculant Adsorption Efficiency, E_F, %	Number of Percentage Units Change
I	0.05	59	+7	1	+18	95	-9	100	-6
II	0.10	66		19		86		94	

have been due to the 9% decrease in mixing efficiency, E_n, or as a result of an optimal quantity of RMD-30 being adsorbed by the mud particles. Although the adsorption efficiency decreased, more RMD-30 was adsorbed per unit area of the mud particles which resulted in the formation of more polymer bridges (and less of polymer molecules adsorbed back unto the same particle) and therefore larger networks. At the higher flocculant dose employed, a three-fold increase in the size of flocs in the zone-settling region was observed, which confirms the presence of larger networks in the compression bed. It is possible that the increase in separation efficiency may also have been due to the larger floc network facilitating the escape of liquid from the bed.

Very few researchers have examined the quantitative effect of a flocculant in thickening. Of these, Wright and Kitchener (1976) using "Laponite" synthetic clay suspensions in a modified laboratory membrane pressure filter showed that for a 40 kg/m^3 suspension, a 400% increase of polyethlene oxide (PEO) dosage resulted in a 60% decrease in permeability. As the permeability is a rough measure of the mean square pore diameter, a thickener sludge would result. Although the quantitative results of the red mud - RMD-30 and "Laponite" clay - PEO systems cannot be compared, the general trends can be. Both show an increase in solids concentration with increase in flocculant dosage. Of course the higher the flocculant dosage, the greater the costs (due to pumping and flocculant) and the the poorer the quality of the overflow, which implies the existence of an optimum dosage for each system.

6.2.3 Effect of Diameter to Length (D/L) Ratio and Temperature on the Separation Efficiency

In the foregoing sections, the results discussed concerned experiments conducted on the experimental thickener with mud by-product of bauxite A. This section deals with results obtained from thickeners, with differing dimensions, processing mud from bauxite B. The distinguishing features of these two types of mud are the source of the bauxite. Although the Bayer Process is used to extract alumina from these bauxites, the process conditions are different because of the chemical composition of the ores.

Referring to Table 6-7, the significant increases of the separation efficiencies, η_{REAL} (+40) and η_{PSEUDO} (+50) of thickener 2 over thickener 1 are shown. The solids flux, inlet concentration, type of flocculant and flocculant dose were similar for both; differences lie in the D/L ratio and the temperature of operation. A parallel effect was noted between thickeners 1 and 3 (decantor of Bayer Process Pilot Plant). The underflow solids concentration from thickener 3 (which has a comparable D/L ratio and operational temperature with that of thickener 2) was approximately equal to that of thickener 2. Therefore, the separation efficiences of thickeners 3 and 2 are approximately equal. The most notable difference between thickeners 2 and 3 was that thickener 3 incorporated a slow moving rake. This increase of separation efficiency could be due to:

(a) Unequal D/L Ratio

The larger diameter to length ratio of the thickeners 2 and 3

TABLE 6-7. Effect of Mud Type, Column Dimensions and Temperature of Operation on Separation Efficiency

Characteristics		η_{Real}	No. of Percentage Units Change	η_{Pseudo}	No. of Percentage Units Change	D/L Ratio / Temp. °C
Mud From Bauxite A	Low specific surface area : Required flocculant dose = 0,05 to $\frac{0.10 \text{ kg RMD-30}}{2000 \text{ kg dry mud}}$ Specific Gravity = 2.93 Total Fe_2O_3 = 20%	59-67		1-19		8.8×10^{-3} / 23-31
Mud From Bauxite B	High specific surface area : Required flocculant dose = 0.30 $\frac{\text{kg RMD-30}}{2000 \text{ kg dry mud}}$ Specific Gravity = 3.41 : Slightly higher due to greater Fe_2O_3 content≈ approx. 52%	Thickener 1: 32	+37	8	+49	8.8×10^{-3} / 25-27
		Thickener 2: 69+		57+		3/4+ / 40-85

\+ Results from plant-size thickener processing mud from bauxite B.

facilitates the formation of a cone of mud at the bottom. As there are limits to the angle of repose of the mud in the liquor, the height of the cone in thickeners 2 and 3 would have been greater. This cone of mud directly influences the separation efficiency due to the mud sloughing off periodically. This mud from the cone is thicker than elsewhere in the thickener as its residence time is longer, also it is postulated that the mud which sloughs off cuts off existing short circuit currents between the feed well and the underflow outlet (which tend to decrease the separation efficiency). The slow-moving rake in thickener 3 may have aided the thickening of the bed by either of or a combination of the following mechanisms:

(1) Breakdown of interparticle polymer bridges,

(2) The cutting off of short circuit routes between the feed well and the underflow outlet, and,

(3) The creation of vertical channels along the stirrer device where liquid preferentially channels upwards.

(b) Solids Flow Pattern

The solids flow pattern in thickener 1 is a plug flow one while that in thickener 2 is as shown in Figure 2-2. So as there is a difference, the process occurring in thickener 1 probably would not simulate those of thickener 2 and dissimilar separation efficiencies would result. This view is supported by Dixon (1980) who states that scale-up of pilot thickeners would be difficult because the flow pattern is expected to be different in different diameter thickeners.

(c) Temperature of Operation

The higher operational temperature of thickeners 2 and 3 may facilitate the dewatering of the bed and/or the collapse of the inter-particle polymer bridges. Dewatering of the bed would be made easier as the viscosity of the liquid is less at a higher temperature. The breakdown of polymer bridges would be promoted at higher temperatures as the decomposition of a synthetic flocculant is faster at higher temperatures.

Considering all of the above factors, it is thought that the D/L ratio and the operational temperature are the most significant which influence the separation efficiency.

6.2.4 Effect of Dry Solids Weight in Bed on the Interface Subsidence Rate

This effect shown in Table 6-8 is significant as a 7% increase in the weight of dry solids (at a similar flocculant dose) resulted in a 73% decrease in the initial settling rate of the bed. Run I which was conducted with a flocculant dosage 50% lower than Runs II and III, had a lower initial weight of dry solids than Runs II and III, subsided at a faster rate. This trend is to be expected as the greater the solids concentration, the larger the resistance to filtration of the liquid. This increased resistance is due to increased drag forces on the fluid by the particles.

Many researchers, who include Maude and Whitmore (1958) and Richardson and Zaki (1954b), have examined the settling rate of a

TABLE 6-8. Initial Rate of Interface Fall as a Function of Dry Solids Present

Run	Flocculant Dose kg RMD-30 / 2000 kg dry mud	Steady State Weight of Dry Mud in Bed kg	Percentage Increase		Initial Rate of Slurry-Supernatant Interface Fall m/hr *	Percentage Decrease	
I	0.05	20.4	24.5	16.7 (I & III)	0.36	91.7	69.4 (I & III)
II	0.10	25.4	-6.3		0.03	-266.7	
III	0.10	23.8			0.11		

* After Removal of Approximately 6 L of Sample Mud

suspension as a function of its concentration. But their results pertain to the zone settling region. Nevertheless, the trend is the same - decreasing settling rates with increasing suspension concentration.

6.2.5 Effect of Flocculant Dose and Solids Concentration on the Compression Point of Mud from Bauxite A

This is discussed as a matter of interest as it is realized that the "compression point" identified may not be the point below which the solids are in compression. Also, this is an inaccurate method for design.

On one hand, considering the 1 to 2% limits of accuracy, there was a negligible change in compression point with increase in solids concentration and flocculant dose. On the other hand, there was a significant increase in settling rates with increase in flocculant dose at different initial solids concentration. This observation is similar to that of Tomalin (1938) and Chakravarti and Dell (1969). Tomalin (1938) using a coal-natural polymer system showed that the sedimentation rate increased with dosage to an optimum polymer concentration, then decreased. Chakravarti and Dell (1969) who conducted experiments with a clay-synthetic polymer system showed that the rate of settling increased with polymer dosage. The effect of dosage was great at high dilutions of the clay system but negligible at low ones.

CHAPTER 7

CONCLUSIONS

This chapter is divided into three parts; the first deals with conclusions that confirm past results, the second with those that are contrary to past findings and the third presents new conclusions.

7.1 Confirmations

7.1.1 Effect of Flocculant Dose on the Separation Efficiency

An increase in the synthetic flocculant dose resulted in an increase in the separation efficiency. This result is in agreement with those of Wright and Kitchener (1976) who obtained a similar trend experimenting with a polyethylene oxide (PEO)-synthetic clay system.

7.1.2 Effect of Flocculant Dose on Settling Rates in the Zone Settling Region

An increase in the synthetic polymer dose increased the settling rate of the red mud suspension. This effect was greater at higher dilutions of the red mud suspension. These findings are similar to that of Chakravarti and Dell (1969).

7.2 Refuting Conclusion

7.2.1 Effect of Solids Throughput on the Separation Efficiency

A decrease in solids throughput resulted in a negligible change in the real separation efficiency and a decrease in the pseudo separation efficiency. This is unlike conventional results where a decrease in solids throughput produces the opposite effect in thickening. Comings et al (1954) and Kos (1977) using different sludges showed that the underflow solids concentration increased when the solids throughput was decreased. The author's anomalous result is attributed to different conditions between tests.

7.3 New Conclusions

7.3.1 Effect of Diameter to Length (D/L) Ratio and Temperature on the Separation Efficiency

An eighty-fold increase in D/L ratio coupled with a two-fold increase in operational temperature had a positive significant effect on the separation efficiency.

7.3.2 Effect of Dry Solids Weight in Bed on Initial Settling Rate

A direct relationship exists between the weight of solids present in the bed at equilibrium and the initial rate of fall of the slurry-supernatant interface at zero throughput. It was found that the greater the quantity of dry solids initially present, the slower the rate of fall of the interface.

CHAPTER 8

RECOMMENDATIONS FOR FURTHER WORK

8.1 Practical Applications

The results of the tests with the misaligned column showed a steep increase in solids concentration with depth just before the angular joint. These results suggest that baffles within a plant-size thickener be used to improve the separation efficiency. The practical problem is that baffles and other objects scale up at a rapid rate in the red mud/liquor system.

The separation efficiency may be affected by alternative draw-off sites (besides the conventional one) which is worth examining. Investigation of alternate outlet routes for the thickened mud with one outlet at the bottom and the other at the side is recommended. This should not necessarily be limited to only two alternate draw-off points.

From observations of the experimental column (thickener 1) and the decantor (thickener 3) in the Bayer Pilot Plant, the effect of a 9 m mud bed is negligible for the experimental column with a D/L ratio of 8.8×10^{-3}. In fact, the greatest increase of solids concentration (apart from the region of column misalignment) occurred in the mud bed just above the underflow outlet. The solids concentration profiles observed by Kos (1977) in a column of D/L ratio 12.5×10^{-2} exhibited

similar trends. The effect of larger D/L ratios on this phenomenon is unknown. Therefore, it is recommended that this be examined as these findings suggest that it may not be economically feasible to build a thickener to accommodate a mud bed greater than a certain height. Of course, if a feasible height does exist, it would vary with the mud type.

The combined factors of a larger D/L ratio and higher temperature of operation increased the real and pseudo efficiencies by 37 and 49%, respectively. It is unknown which factor had the more significant effect. Therefore, it is recommended that this be investigated.

For each thickener system, experiments should be conducted to determine the optimum polymer dose to minimize polymer cost.

REFERENCES

1. Adorján, L. A. (1975), "A Theory of Sediment Compression", paper presented at Eleventh International Mineral Processing Congress, Cagliari, Italy.

2. Adorján, L. A. (1976), Trans. Inst. Mining and Metall., 85, C157.

3. Bonjer, J., Clement, M. (1974), Erzmetall., 27, 475.

4. Chakravarti, A., Dell, C. C. (1969), Pouder Tech., 3, 287.

5. Chandler, J. L. (1976), "Design of Deep Thickeners", paper presented at the Institution of Chemical Engineers' "Design '76 Congress", Birmingham, England.

6. Coe, H. S., Clevenger, G. H. (1916), Trans. A.I.M.E., 55, 356.

7. Comings, E. W. (1940), I. & E. C., 32, 663.

8. Comings, E. W., Pruiss, C. E., Debord, C. (1954), Ind. Eng. Chem., 46, 1164.

9. Couchè, R. A., Goldney, L. M. (1959), Proc. Aust. I. M. M., 191, 117.

10. Deane, W. A. (1920), Trans. Am. Electrochem. Soc., 37, 71.

11. Dell, C. C., Keleghan, W. T. H. (1973), Pouder Tech. 7, 189.

12. Dell, C. C., Sinha, J. (1966), Trans. Inst. Mining Metall., 75, C139.

13. Dixon, D. C. (1977b), Sep. Sci. Tech., 12, 193.

14. Dixon, D. C. (1978), Sep. Sci. Tech., 13, 753.

15. Dixon, D. C. (1980), A. I. Ch. E., 26, 471.

16. Fitch, B. (1962), Ind. Eng. Chem., 54, 44.

17. Fitch, B. (1966a), Ind. Eng. Chem. Fund., 5, 129.

18. Fitch, B. (1966b), Ind. Eng. Chem. 58 (10), 18.

19. Fitch, B. (1979), A. I. Ch. E., 25, 913.

20. Happel, J., Brenner, H. (1973), "Low Reynolds Number Hydrodynamics", 2nd. rev. ed., p. 387, Noordhoff International Publishing, Holland.

21. Harris, C. C., Somasundaran, P., Jensen, R. P. (1975), Powder Technol., 11, 75.

22. Hassett, N. J. (1958a), Ind. Chem., 34, 116.

23. Hassett, N. J. (1958b), Ind. Chem., 34, 169.

24. Hassett, N. J. (1958C), Ind. Chem., 34, 489.

25. Hassett, N. J. (1964), Ind. Chem., 40, 29.

26. Kalbskopf, K. H. (1972), Water Res., 6, 499.

27. Kynch, G. J. (1952), Trans. Farad. Soc., 48, 166.

28. Kos, P. (1977), Prog. Water Tech., 9, 291.

29. Kos, P., Adrian, D. D. (1975), J. Environ. Eng. Div. Am. 101, 947.

30. Le Clair, B. P., Hamielec, A. E. (1969), Ind. Eng. Chem. Fund., 7, 542.

31. Maude, A. D., Whitmore, R. L. (1958), Br. J. Appl. Phys., 9, 477.

32. Michaels, A. S., Bolger, J. C. (1962), I. and E. C. Fund. 1, 24.

33. Panov, A. S., Kuznetsov, S. I. (1973), Izv Vyssh Ucheb Zaved Tsvet Metall. 5, 57.

34. Richardson, J. F., Zaki, W. N. (1954b), Chem. Eng. Sci. 3, 65.

35. Roberts, E. J. (1934), Trans. A. I. M. E. 112, 178.

36. Roberts, E. J. (1949), Min. Eng. 1, 61.

37. Scandrett, H. F. (1963), Extractive Metallurgy of Aluminum, Vol. I, Alumina, p. 85, ed. Gerand, G. and Stroup, P. T., Interscience Publ., N.Y.

38. Scott, K. J. (1965a), Trans. Inst. Mining Metall., 74, C627.

39. Scott, K. J. (1968a), Trans. Inst. Mining Metall., 77, C85.

40. Scott, K. J. (1968b), Ind. Eng. Chem. Fund. 7, 484.

41. Scott, K. J. (1968c), Ind. Eng. Chem. Fund. 7, 582.

42. Shannon, P. T., Tory, E. M. (1966), Trans. A. I. M. E., 235, 375.

43. Shin, B. S. and Dick, R. I. (1975), Prog. Water Tech., 7, 137.

44. Smiles, D. E. (1976), Sep. Science, 11, 1.

45. Stinson, J. M. (1979), "Red Mud Lake Simulation", paper presented at the 108th Annual Meeting of the A. I. M. E., New Orleans, Louisiana.

46. Talmage, W. P., Fitch, E. B. (1955), I. E. C., 47, 38.

47. Tomalin, E. F. (1938), Trans. Inst. Chem. Eng., 16, 231.

48. Wright, H. J. L., Kitchener, J. A. (1976), J. Coll. I. Sc., 56, 57.

49. Yoshioka, N. et al (1955), J. Chem. Soc. Jap., 19, 616.

APPENDIX A. Preparations, Test Procedures and Equipment

A.1 Preparation of Stock RMD-30 Solution

A solution of 0.25% strength was prepared as follows: a weighed quantity of RMD-30 was transferred to a completely dry bottle, this was wetted by adding 3 cm^3 of ethyl or methyl alcohol per gm of powder, then the correct volume of distilled water was rapidly poured on - immediately the vessel was closed and agitated vigorously for 30 seconds. Further agitation during the next 60 minutes completed the dissolution.

This initial solution was diluted to 0.025% to provide a working strength solution.

A.2 Test for Residual Synthetic Flocculant in Overflow Liquor

A 20 ml sample of the overflow liquor was filtered on a Gelman Instrument Company glass fibre filter type A (47 mm) at 250 mm Hg vacuum. From the filtration time, the concentration of the synthetic flocculant was determined from the calibration curve. The calibration curve was obtained by noting the filtration times of 20 ml volumes at 250 mm Hg vacuum of a similar suspension made with liquor of the same concentration but with known concentrations of RMD-30 synthetic flocculant.

A.3. Photographs of Equipment

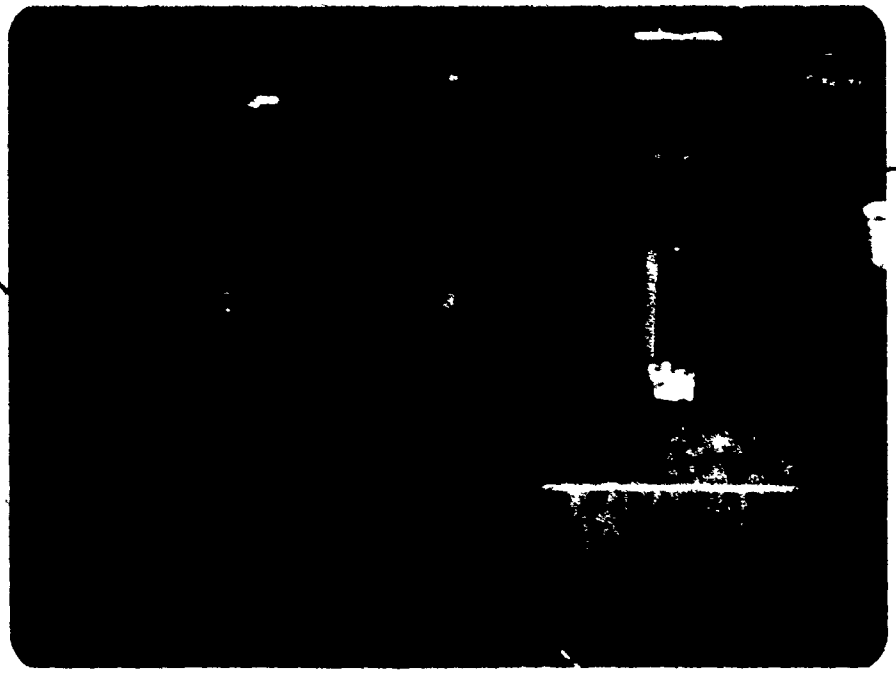

FIGURE A-1. Photograph of Feed Assembly

FIGURE A-2. Photograph of Feed Assembly Showing T-Joint Where Mixing Occurred

FIGURE A-3. Photograph of Discharge Collection Area

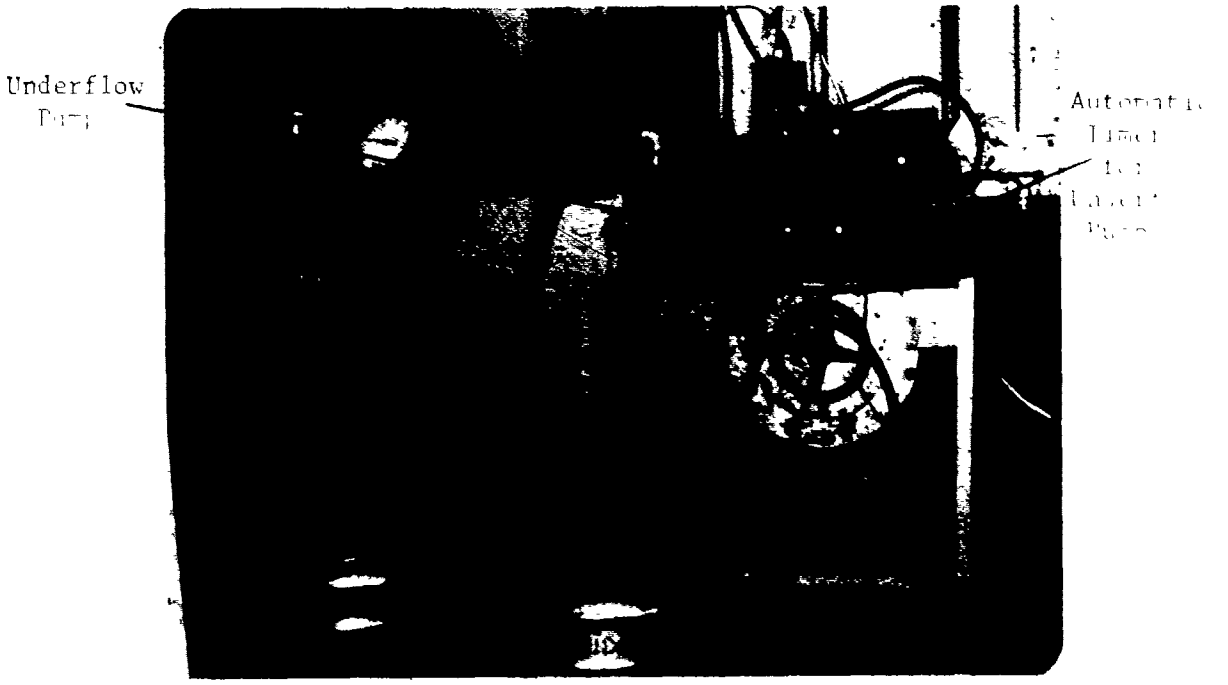

FIGURE A-4. Photograph of Column While Underflowing

APPENDIX B. Mud Characterisation Analytical Results

B.1. Characterisation of Mud from Bauxite A

TABLE B-1. Physical Mud Characteristics - Mud Processed from Bauxite A

Drum No.	Density g/cm^3	Surface Area* m^2/g (1 hr. Degas at 105°C)
A-1	2.93	18.7
A-2	2.93	17.2
A-3	2.93	18.5
A-4	2.93	17.9
A-5	2.92	20.0
A-6	2.95	18.6
Average	2.93	18.5

* Total of external and pore surface area by nitrogen adsorption methods.

TABLE B-2. Particle Size Distribution - Mud Processed from Bauxite A

Sample from Drum No.	% Less than Certain Size in Microns													
	250*	149*	105*	74*	53*	45*	33+	20+	10+	7+	5+	3+	2+	1+
A-1	98.8	96.9	93.2	90.7	89.5	89.0	87.8	84.7	80.0	77.0	74.0	63.5	51.0	26.0
A-2	99.5	98.5	97.0	95.0	93.2	92.3	91.5	89.0	83.7	80.2	75.0	60.0	41.0	11.0
A-3	99.8	98.0	95.7	94.4	93.3	92.7	91.0	87.0	80.0	76.5	72.5	63.0	47.0	19.0
A-4	99.9	99.2	98.6	97.7	96.5	95.7	94.4	91.0	83.5	78.5	72.0	58.0	43.0	16.5
A-5	99.7	98.4	97.2	95.7	94.8	94.2	92.5	88.5	81.5	77.0	72.0	59.0	47.0	29.0
A-6	99.8	98.7	97.3	95.8	94.3	93.5	91.8	88.5	82.0	78.0	72.5	59.0	43.0	13.5

* Analysed by wet screening

\+ Analysed by centrifugation

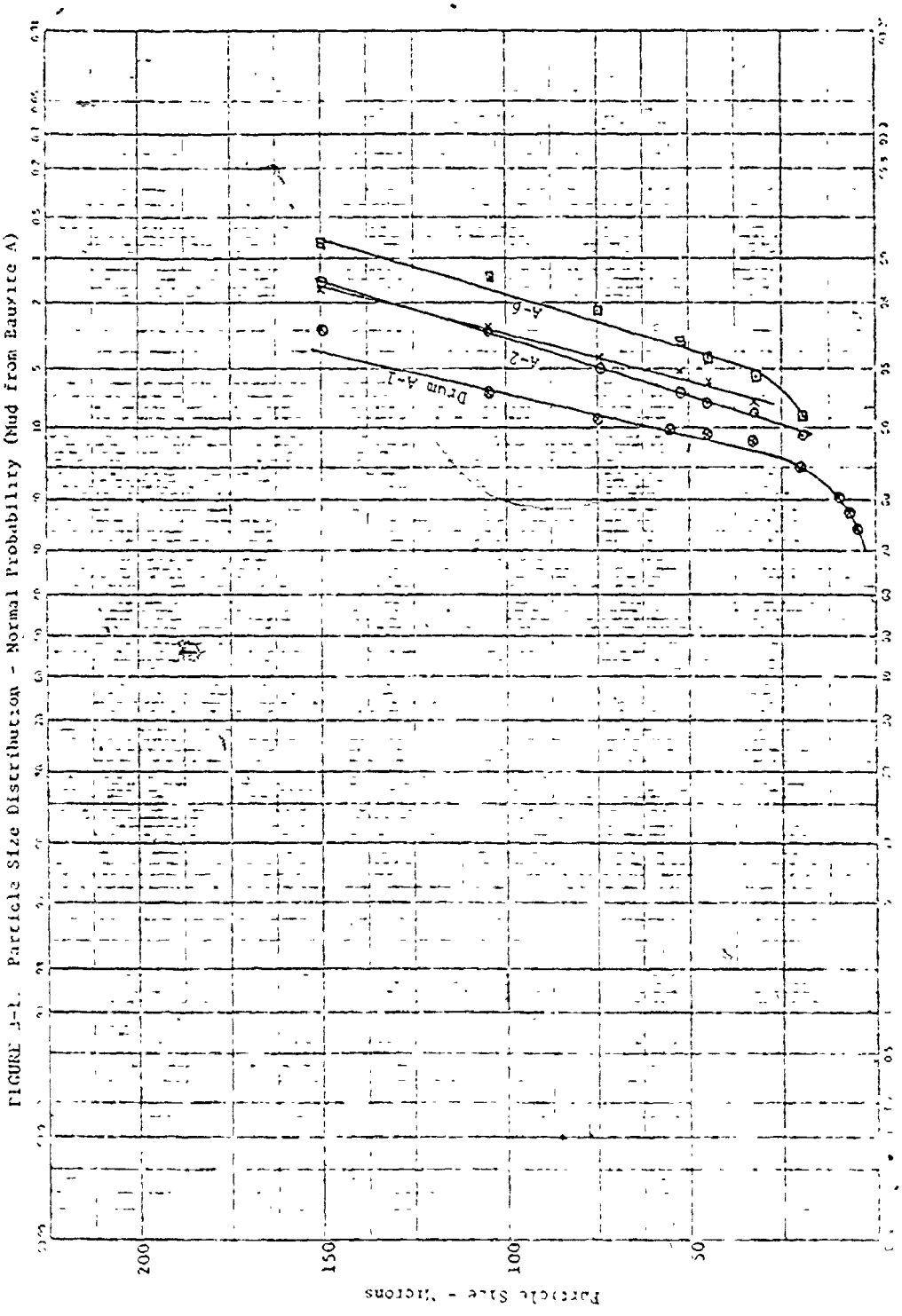

FIGURE J-1. Particle Size Distribution - Normal Probability (Mud from Bauxite A)

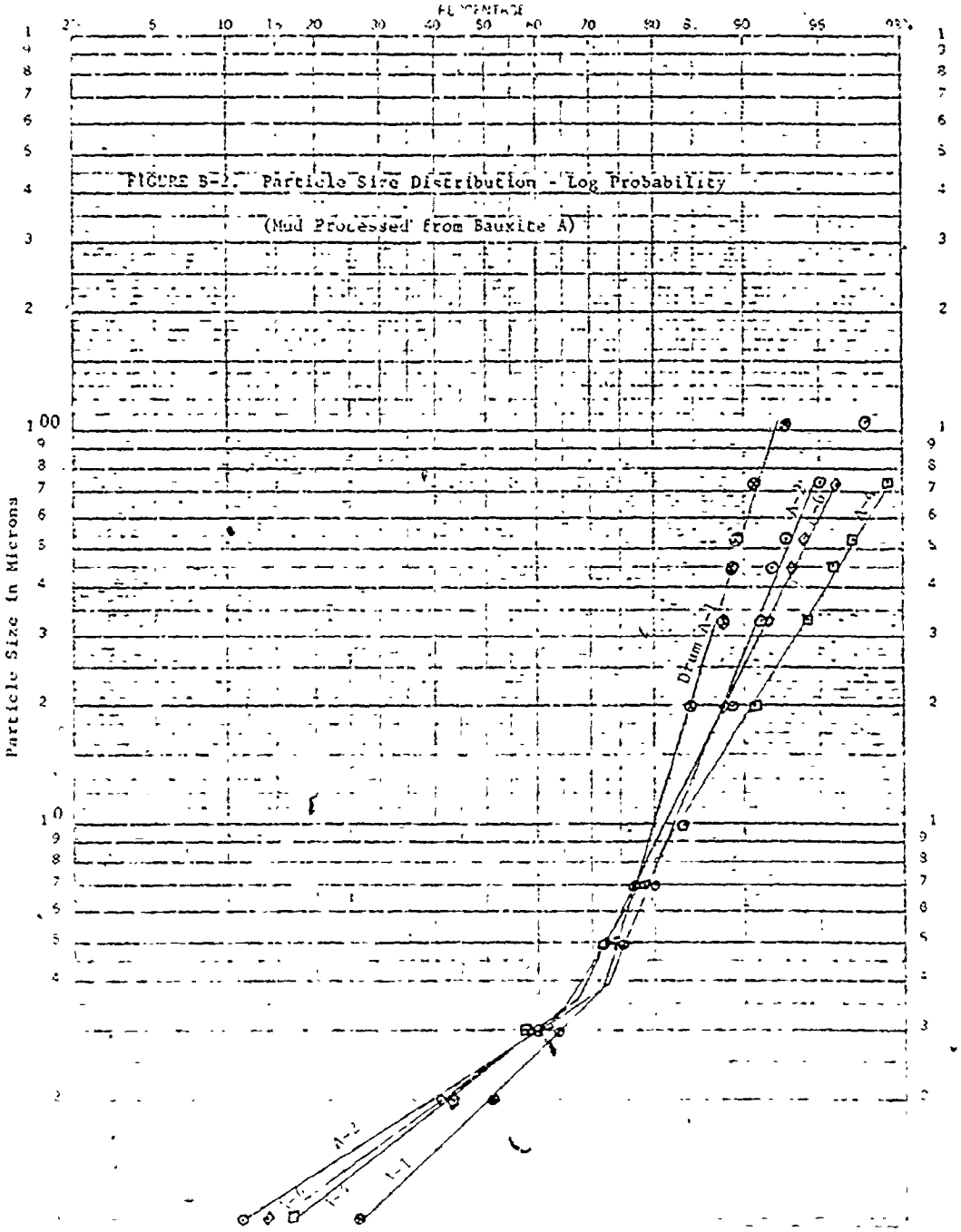

FIGURE B-2. Particle Size Distribution - Log Probability

(Mud Processed from Bauxite A)

B.2. Characterisation of Mud from Bauxite B

TABLE B-4. Particle Size Distribution for Mud Processed from Bauxite B

Percentage Less Than Certain Size in Microns														
Sample from Drum No.	149*	105*	74*	53*	44*	30++	20++	10++	7++	5++	4++	3++	2++	1++
B-1	99.1	99	98.4	98.0	97.3	83,0	68.0	46.0	37.0	31.0	26.5	21.0	15.0	7.8
B-2	99.5	98.8	98.6	98.3	97.6	86.5	79.0	66.0	60.0	55.0	51.5	47.0	40.5	26.0
B-3	99.3	99.0	98.7	98.4	97.7	88.0	75.0	60.0	56.5	49.0	45.0	40.0	33.0	23.0

* Analysed by Wet Screening

++ Analysed by Centrifugation

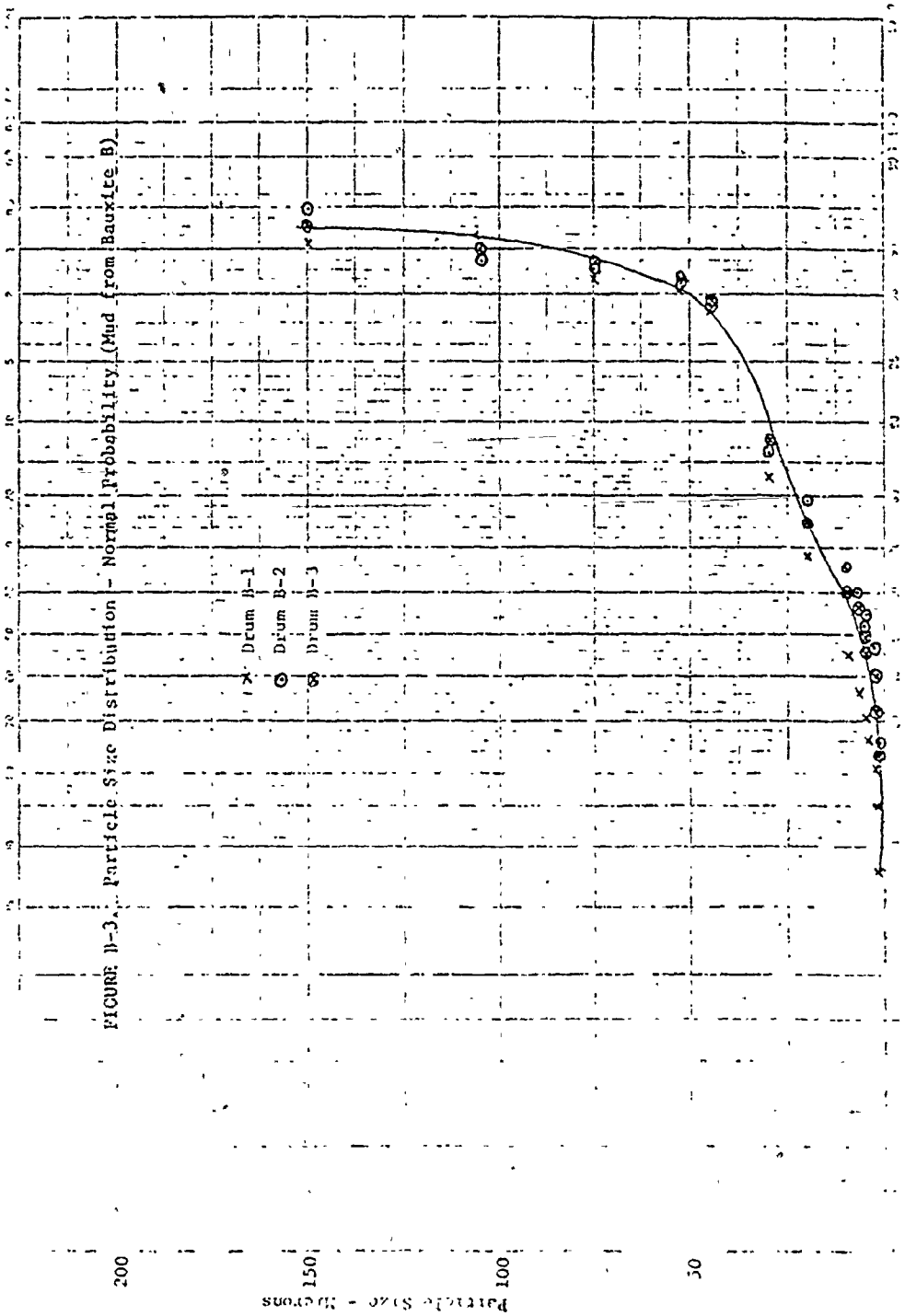

FIGURE B-3. Particle Size Distribution - Normal Probability (Mud from Bauxite B)

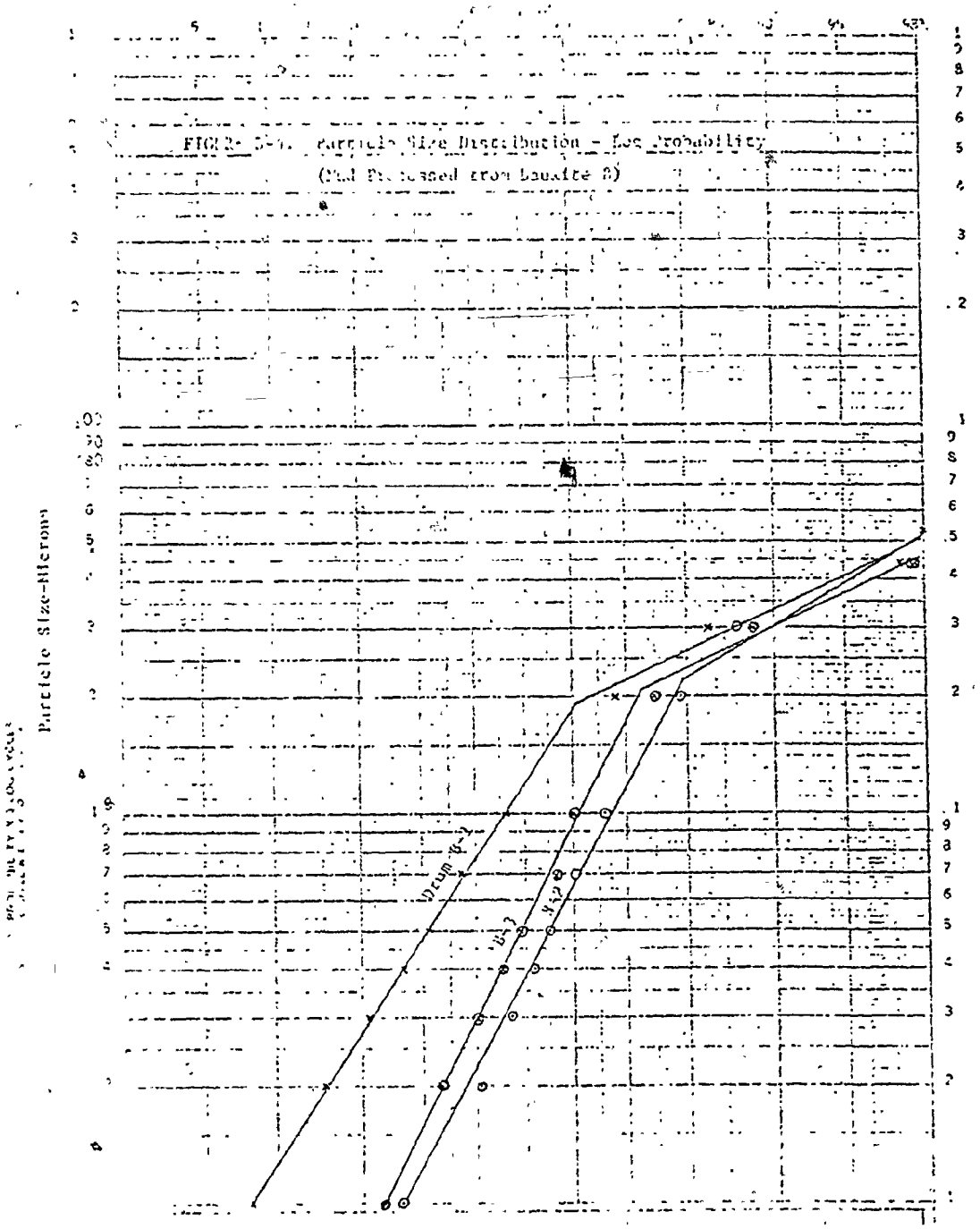

FIGURE 5-4. Particle Size Distribution - Log Probability
(Pilot Processed from Bauxite B)

TABLE B-5. Quantitative Analyses and Physical Characteristics of Mud Processed From Bauxite B

Drum No.	Specific Gravity	Surface Area*	Total				Loss on Ignition (L.O.I.) %	Goetite / Hematite Ratio	SO_2 Soluble			
			SiO_2 %	Fe_2O_3 %	TiO_2 %	Al_2O_3 %			Al_2O_3 %	SiO_2 %	CaO %	Na_2O %
B-1	3.43	78.3	1.98	52.5	7.5	13.78	11.98	60/40	1.50	1.31	5.53	1.19
B-2	3.39	62.4	1.90	52.3	7.4	13.92	11.41	61/39	1.53	1.33	5.56	1.17
B-3	3.42	66.8	2.06	52.7	7.4	14.18	11.23	60/40	1.53	1.28	5.65	1.08
Average	3.41	69.2										

* Total of external and pore surface area (by nitrogen adsorption)

APPENDIX C. Experimental Results

LEGEND

T.T.S. ≡ Total Titratable Soda

C.1. Results of Experimental Runs

TABLE C-1. Run I: Feed Slurry Analytical Results

Time of Operation + hr	10.0	12.0	14.0	16.0	18.0	20.0	22.0
Solids Concentration %	27.6	28.3	27.1	27.6	27.6	27.8	27.9
Temperature ^{o}C ±0.5	27	25	24.5	24.5	25	25	24.5

Time of Operation + hr.	Solids Concentration % ±0.6	Liquor Density g/cm^3	Caustic Concentration g/L * ±0.4	Al_2O_3 Concentration g/L ±0.3	Ratio $\frac{Al_2O_3}{Caustic}$ ±0.001	T.T.S. Concentration g/L ±0.5	Causticity $\frac{Caustic}{TTS} \times 100$ %
22.75	27.9	1.03	14.5	4.5	0.310	24.2	59.9

+ After commencement of underflowing

* Expressed as equiv. Na_2CO_3

TABLE C-2. Run I: Overflow Analytical Results

Time of Operation+ hr	Clarity mg/L	Temp. °C ±0.5	Liquor Density g/cm³	Caustic Concentration g/L* ±0.4	Al_2O_3 Concentration g/L ±0.3	Ratio $\frac{Al_2O_3}{Caustic}$ ±0.001	T.T.S. Concentration g/L ±0.5	Causticity $\frac{Caustic}{T.T.S.} \times 100$ %	Residual Flocculant Average Filtration Time SEC
16.5	101	25	1.01	6.7	1.7	0.254	9.5	70.5	
18.5	92	25	1.01	6.7	1.7	0.254	9.5	70.5	1.5
20.5	99	25	1.01	5.4	1.2	0.222	7.1	76.1	
22.5	110	25	1.01	6.7	1.7	0.254	8.9	75.3	1.4
22.75		24.5	1.01	6.7	1.7	0.254	9.0	74.4	

+ After commencement of underflowing

* Expressed as equiv. Na_2CO_3

TABLE C-3. Run I: Underflow Slurry Analytical Results

Time of Operation+ hr	Solids Concentration % ±0.6	Time of Operation+ hr	Solids Concentration % ±0.6	Caustic Concentration g/L* ±0.4	Al_2O_3 Concentration g/L ±0.3	Ratio $\frac{Al_2O_3}{Caustic}$ ±0.001	T.T.S. Concentration g/L ±0.5	Causticity = $\frac{Caustic}{T.T.S.}$ x 100 %	Temp. ^oC	Liquor Density g/cm^3
1.5	49.7	14.5	30.7	8.7	2.1	0.241	11.8	73.7	25	1.01
2.5	38.8	15.5	32.4	9.3	2.0	0.215	12.2	76.2	25	1.01
3.5	34.8	16.5	30.2	8.2	1.9	0.232	10.9	75.2	25	1.01
4.5	33.3	17.5	28.6	7.4	1.8	0.243	10.2	72.5	25	1.01
5.5	38.1	18.5	28.7	7.0	1.7	0.243	10.1	69.3	25	1.01
6.5	37.1	19.5	28.3	7.3	1.7	0.233	10.0	73.0	25	1.01
7.5	33.1	20.5	28.1	6.9	1.7	0.246	9.9	69.7	25	1.01
8.5	33.3	21.5	27.4	7.1	1.7	0.239	9.7	73.2	25	1.01
9.5	32.2	22.5	28.0	6.9	1.8	0.265	9.7	71.1	24	1.01
10.5	31.7									
11.5	30.9									
12.5	31.7									
13.5	31.5									

\+ After commencement of underflowing

* Expressed as equiv. Na_2CO_3

TABLE C-4. Run II: Feed Slurry Analytical Results

Time of Operation+ hr	Solids Concentration % ±0.6%	Caustic Concentration g/L * ±0.4	Al_2O_3 Concentration g/L ±0.3	Ratio $\frac{Al_2O_3}{Caustic}$ ±0.001	T.T.S. Concentration g/L ±0.5	Causticity = $\frac{Caustic}{T.T.S.} \times 100$ %	pH	Temperature ^oC ±0.5
12.5	27.9	18.5	3.2	0.17	24.7	74.9	12.9	28
14.5	28.4	18.4	3.0	0.16	24.4	75.4	13.0	28
16.5	27.9	19.5	3.8	0.19	24.5	79.6	12.9	27.5
18.5	28.8	19.1	3.8	0.20	24.4	78.3	12.9	27.5
20.5	28.5	18.9	3.3	0.17	24.1	78.4	12.9	27
22.5	29.1	18.3	3.0	0.16	24.4	75.0	12.9	27

+ After commencement of underflowing

* Expressed as equiv. Na_2CO_3.

TABLE C-5. Run II: Overflow Analytical Results

Time of Operation+ hr	Clarity mg/L	Caustic Concentration g/L* ±0.4	Al_2O_3 Concentration g/L ±0.3	Ratio $\frac{Al_2O_3}{Caustic}$ ±0.001	T.T.S. Concentration g/L ±0.5	Causticity = $\frac{Caustic}{T.T.S.}$ x100 %	pH	Residual Flocculant Filtration Time SEC	Temp. ^oC ±0.5
15.5	165	7.5	1.3	0.17	8.5	88.2	12.4	2.2	25
17.5	97	7.5	1.3	0.17	8.6	87.2	12.4	2.9	25
19.5	104	7.3	1.2	0.16	9.3	78.5	12.4	2.6	25
21.5	109	7.0	1.1	0.16	8.6	81.4	12.4	2.7	24
22.5	105	7.5	1.1	0.15	9.1	82.4	12.4	3.0	25

+ After commencement of underflowing

* Expressed as equiv. Na_2CO_3

TABLE C-6 Run II: Underflow Slurry Analytical Results

Time of Operation + hr	Solids Concentration %	Time of Operation + hr	Solids Concentration % ±0.6	Caustic Concentration g/L* ±0.4	Al_2O_3 Concentration g/L ±0.3	Ratio $\frac{Al_2O_3}{Caustic}$ ±0.001	T.T.S. Concentration g/L ±0.5	Causticity = $\frac{Caustic}{T.T.S.} \times 100$ %	pH	Temperature °C ±0.5
11.5	43.3	12.5	31.5	9.2	1.6	0.17	10.4	88.5	12.5	24
2.5	44.3	13.5	31.4	8.4	1.5	0.18	11.2	75.0	12.5	24
3.5	41.6	14.5	31.3	8.4	1.5	0.18	11.2	75.0	12.5	24
4.5	38.1	15.5	30.0	8.9	1.4	0.16	10.7	83.2	12.5	24
5.5	41.5	16.5	30.7	8.3	1.7	0.20	11.2	74.1	12.4	24
6.5	41.0	17.5	31.7	9.3	1.6	0.17	11.4	81.6	12.5	24
7.5	39.2	18.5	31.4	9.0	1.3	0.14	11.6	77.6	12.5	24
8.5	34.2	19.5	32.0	8.3	1.4	0.17	11.4	72.8	12.5	24
9.5	31.2	20.5	31.8	8.5	1.4	0.16	10.4	81.7	12.5	23
10.5	32.2	21.5	33.8	8.8	1.2	0.14	10.4	84.6	12.5	23
11.5	30.5	22.5	34.8	8.5	1.3	0.15	10.3	82.5	12.4	23
sample from Valve #2		19.5	37.0							

+ After commencement of underflowing

* Expressed as equiv. Na_2CO_3

TABLE C-7. Run II: Particle Size Analyses as a Function of Depth at Steady State

Sample Port No.	Height above U/F m	% Less Than A Certain Size In Microns													
		149*	105*	74*	53*	44*	30++	20++	10++	7++	5++	4++	3++	2++	1++
1	0.91	97.2	95.1	93.3	92.2	92.0	91.5	88.5	81.5	77.5	72.0	67.0	58.0	42.0	19.5
2	1.83	97.3	95.5	93.7	92.0	91.1	90.3	88.3	80.0	75.0	70.0	66.0	57.0	39.0	14.0
3	2.74	97.7	96.4	94.7	92.8	92.2	91.0	88.5	79.5	73.5	67.0	62.5	55.0	37.0	15.0
4	3.66	96.2	94.7	93.0	91.7	91.4	91.0	88.0	80.0	75.5	66.0	56.0	46.0	39.0	14.5
5	4.88	97.3	96.3	94.7	92.8	92.0	91.0	89.2	81.5	77.0	71.5	67.5	59.0	42.0	15.5
6	6.10	98.4	95.5	93.7	92.3	91.9	91.0	89.0	81.5	76.5	70.5	67.5	59.0	44.0	17.0
7	7.31	97.3	95.8	94.2	92.0	90.5	89.5	88.1	81.0	76.5	72.0	67.0	59.0	42.0	15.5
8	8.55	97.7	96.0	94.4	93.2	92.5	91.0	87.9	81.0	77.0	71.0	66.5	58.0	41.0	15.5

* Micromesh sieves

++ Analyzed by centrifugation

U/F Underflow

TABLE C-8. Run III: Feed Slurry Analytical Results

Time of Operation+ hr	Solids Concentration %	Liquor Density g/cm^3	Caustic Concentration g/L* ±0.4	Al_2O_3 Concentration g/L ±0.3	Ratio $\frac{Al_2O_3}{Caustic}$ ±0.001	T.T.S. Concentration g/L ±0.5	Causticity = $\frac{Caustic}{T.T.S.} \times 100$ %	pH	Temp. °C ±0.5
-2	27.4	1.02	14.7	4.0	0.27	24.1	61.0	12.9	31
-2	29.6								
6	28.5	1.02	14.8	3.9	0.26	23.5	63.0	12.9	32
10	29.3								
14	27.6	1.02	15.3	3.9	0.25	24.5	62.4	12.9	30
18	29.6								
22	29.0	1.02	14.7	3.9	0.26	23.5	62.6	12.9	27
25	28.5								
28	27.7		14.2	4.0	0.28	24.3	58.4	12.9	26
31	28.5								

+ After commencement of underflowing

* Expressed as equiv. Na_2CO_3

TABLE C-9. Run III: Diluted Feed Slurry Analytical Results

Time of Operation+ hr	Solids Concentration %	Liquor Density g/cm^3	Caustic Concentration g/L* ±0.4	Al_2O_3 Concentration g/L ±0.3	Ratio $\frac{Al_2O_3}{Caustic}$ ±0.001	T.T.S. Concentration g/L ±0.5	Causticity = $\frac{Caustic}{T.T.S.} \times 100$ %
0	10.5	1.01	7.9	1.5	0.19	10.5	75.2
12	13.5						
24	11.5	1.01	7.4	1.4	0.19	9.6	77.1
28	13.6						
32	11.3	1.01	7.3	1.2	0.16	9.4	77.7

+ After commencement of underflowing

* Expressed as equiv. Na_2CO_3

TABLE C-10. Run III - Overflow Analytical Results

Time of Operation + hr	Clarity mg/L	Liquor Density g/cm^3	Caustic Concentration g/L * ±0.4	Al_2O_3 Concentration g/L ±0.3	Ratio $\frac{Al_2O_3}{Caustic}$ ±0.001	T.T.S. Concentration g/L ±0.5	Causticity = $\frac{Caustic}{T.T.S.} \times 100$ %	Temp. ^oC ±0.5
25	263	1.01	6.5	1.1	0.17	10.5	61.9	27
27	150	1.01	5.9	1.3	0.22	9.8	60.2	26
29	174	1.01	5.9	1.4	0.24	10.2	57.8	25
31	137	1.01	5.9	1.3	0.22	9.4	62.8	25

\+ After commencement of underflowing

* Expressed as equiv. Na_2CO_3

TABLE C-11. Run III - Underflow Slurry Analytical Results

Time of Operation+ hr	Solids Concentration %	Time of Operation+ hr	Solids Concentration %	Liquor Density g/cm^3	Caustic Concentration g/L*	Al_2O_3 Concentration g/L ±0.3	Ratio $\frac{Al_2O_3}{Caustic}$ ±0.001	T.T.S. Concentration g/L ±0.5	Causticity = $\frac{Caustic}{T.T.S.}$ x100	pH	Temp. °C ±0.5
0	47.1	16	32.2	1.01	14.6	2.0	0.14	17.3	84.4	13.0	31
2	41.1	18	31.6								
4	40.2	20	31.7	1.01	11.0	1.9	0.17	13.9	79.1	13.0	31
6	39.0	22	32.2								
8	35.5	24	32.5	1.01	7.4	1.9	0.26	11.3	65.5	12.8	27
10	31.7	25	30.9								
12	31.8	26	31.2	1.01	7.8	1.6	0.21	10.6	73.6	12.8	25
14	33.3	27	28.3								
		28	31.2	1.01	8.4	1.4	0.17	11.3	74.3	12.6	25
		29	31.7								
		30	30.4	1.01	8.2	1.3	0.16	10.3	79.6	12.6	26
		31	30.7								

+ After commencement of underflowing

* Expressed as equiv. Na_2CO_3

TABLE C-12. Run IV: Feed Slurry Analytical Results

Time of Operation+ hr	Solids Concentration %	Liquor Density g/cm^3	Caustic Concentration g/L* ±0.4	Al_2O_3 Concentration g/L ±0.3	Ratio $\frac{Al_2O_3}{Caustic}$ ±0.001	T.T.S. Concentration g/L ±0.5	Causticity= $\frac{Caustic}{T.T.S.} \times 100$ %	Temp. ^oC ±0.5
1.5	18.1	1.01	11.4	3.3	0.29	13.9	82.0	27
6.25	18.1							
8.0	17.9							
12.0	18.6	1.01	10.0	3.2	0.32	13.0	76.9	26
15.0	17.6							
20.0	19.1							
22.0	19.0	1.01	10.5	2.9	0.28	13.0	80.8	26
25.0	18.7							
26.0	18.1							

\+ After commencement of underflowing

* Expressed as equiv. Na_2CO_3

TABLE C-13. Run IV - Diluted Feed Analytical Results

Time of Operation+ hr	Solids Concentration %	Liquor Density g/cm^3	Caustic Concentration g/L* ±0.4	Al_2O_3 Concentration g/L ±0.3	Ratio $\frac{Al_2O_3}{Caustic}$ ±0.001	T.T.S. Concentration g/L ±0.5	Causticity = $\frac{Caustic}{T.T.S.} \times 100$ %
1.5	13.9	1.01	8.0	2.3	0.29	10.5	76.2
8.0	13.6						
16.0	13.4	1.01	7.1	1.8	0.25	9.2	77.2
25.0	13.5						

\+ After commencement of underflowing

* Expressed as equiv. Na_2CO_3

TABLE C-14. Run IV: Overflow Analytical Results

Time of Operation+ hr	Clarity mg/L	Liquor Density g/cm^3	Caustic Concentration g/L * ±0.4	Al_2O_3 Concentration g/L ±0.3	Ratio $\frac{Al_2O_3}{Caustic}$ ±0.001	T.T.S. Concentration g/L ±0.5	Causticity = $\frac{Caustic}{T.T.S.} \times 100$ %	Temp. °C ±0.5
18	51	1.004	6.3	1.5	0.24	7.2	87.5	27
20	79							
22	52	1.004	6.2	1.5	0.24	7.2	86.1	27
24	55							

+ After commencement of underflowing

* Expressed as equiv. Na_2CO_3

TABLE C-15. Run IV: Underflow Slurry Analytical Results

Time of Operation + hr	Solids Concentration %	Liquor Density g/cm^3	Caustic Concentration g/L * ±0.4	Al_2O_3 Concentration g/L ±0.3	Ratio $\frac{Al_2O_3}{Caustic}$ ±0.001	T.T.S. Concentration g/L ±0.5	Causticity = $\frac{Caustic}{T.T.S.} \times 100$ %	Temp. ^oC ±0.5
6	20.1	1.01	9.8	2.9	0.29	12.0	81.7	25
8	21.2							
10	20.9							
12	20.3	1.01	9.5	2.6	0.27	11.6	81.9	25
14	19.1							
16	18.8							
18	18.8	1.01	9.8	2.6	0.26	11.5	85.2	27
19	18.8							
20	18.9							
21	18.7	1.01	9.0	2.4	0.27	10.5	85.7	25
22	20.0							
23	20.0							
24	20.2	1.01	8.7	2.4	0.27	10.4	83.6	25
25	19.2							
25.5	20.4							

+ After commencement of underflowing

* Expressed as equiv. Na_2CO_3

TABLE C-16. Bed Height as a Function of Time at Zero Throughput

Run	Time After End of Continuous Run hr	Bed Height m
I	0	8.4
	28	6.13
	52	5.76
	72	5.59
II	0	8.5
	26	7.68
	50	7.22
	74	6.94
	108	6.70
	132	6.51
III	0	8.44
	13	7.56
	21	7.26
	38.5	6.79
	47.5	6.64
	71	6.35
	93	6.14
	120	5.92
	132.5	5.83

C.2. Results of Batch Settling Tests

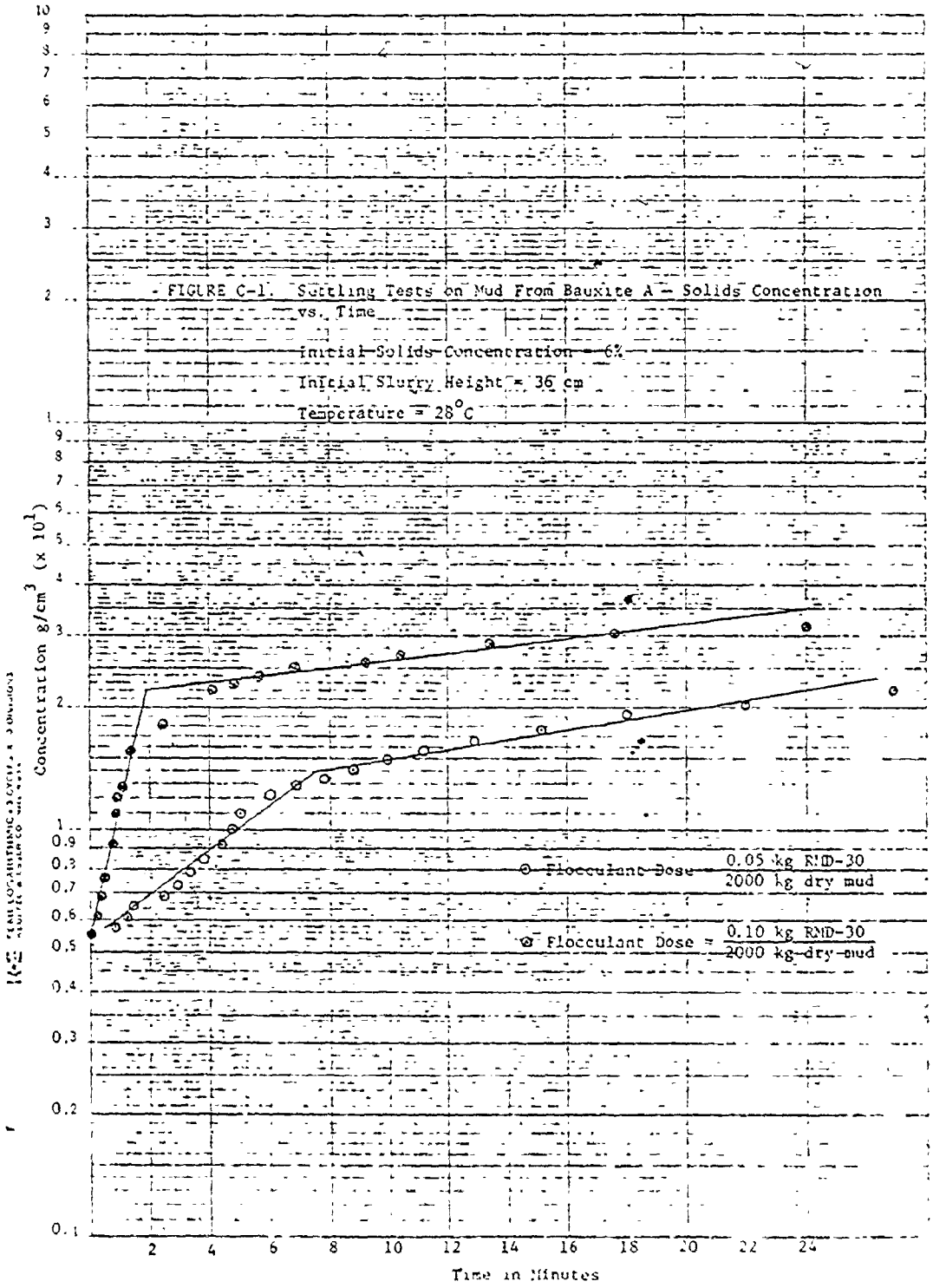

FIGURE C-1. Settling Tests on Mud From Bauxite A — Solids Concentration vs. Time

Initial Solids Concentration = 6%

Initial Slurry Height = 36 cm

Temperature = 28°C

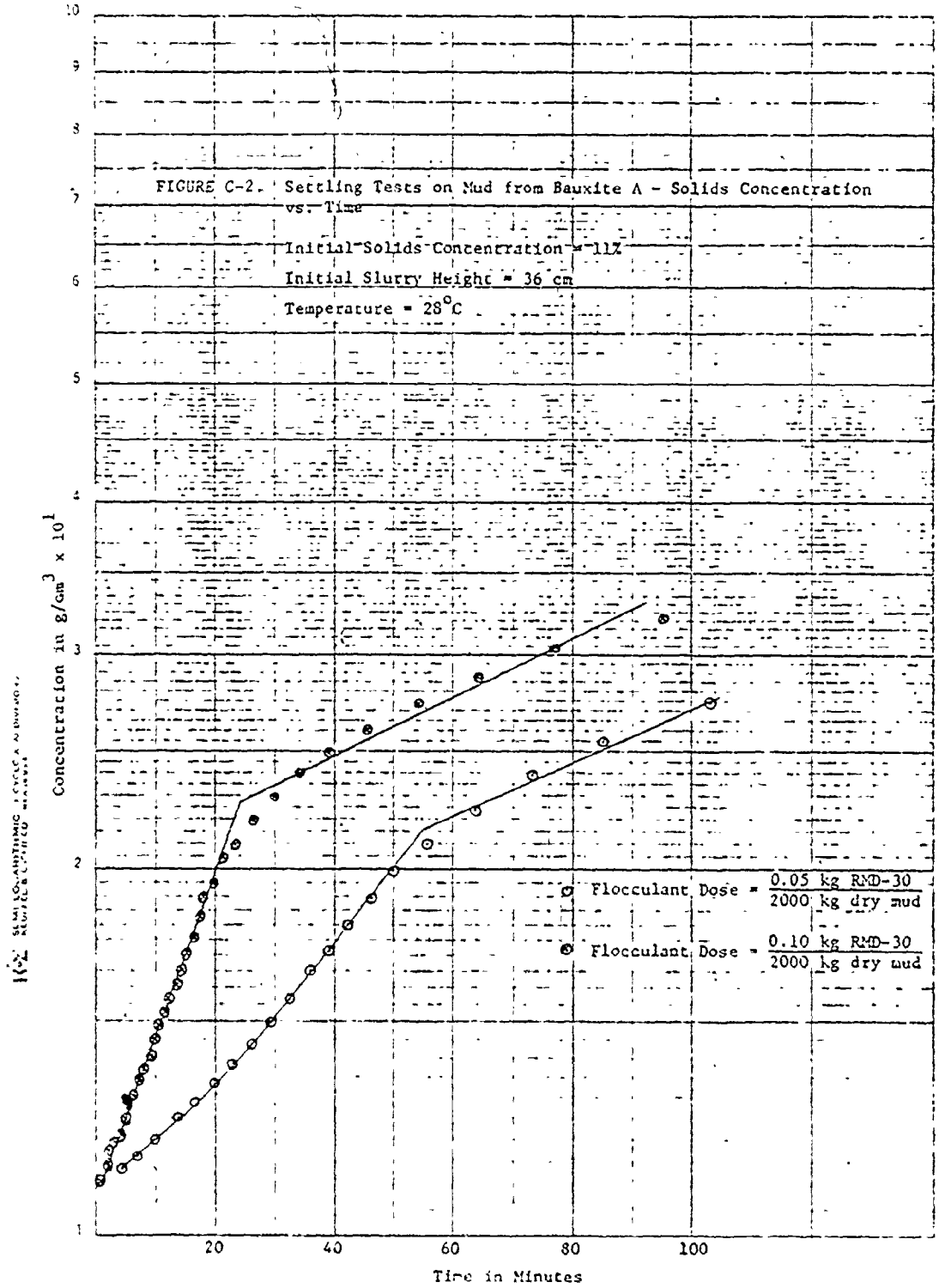

FIGURE C-2. Settling Tests on Mud from Bauxite A - Solids Concentration vs. Time

Initial Solids Concentration = 11%

Initial Slurry Height = 36 cm

Temperature = 28°C

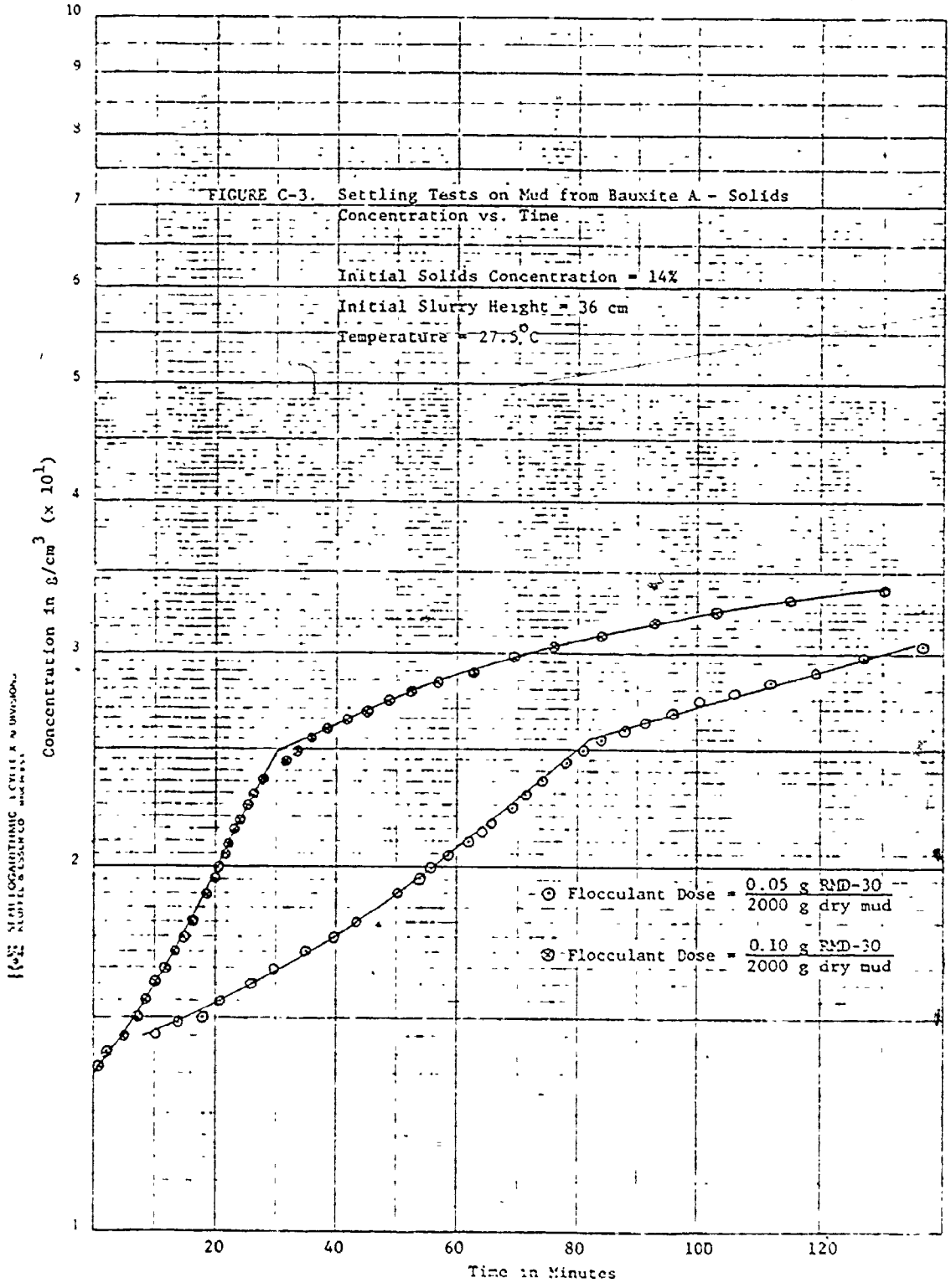

FIGURE C-3. Settling Tests on Mud from Bauxite A - Solids Concentration vs. Time

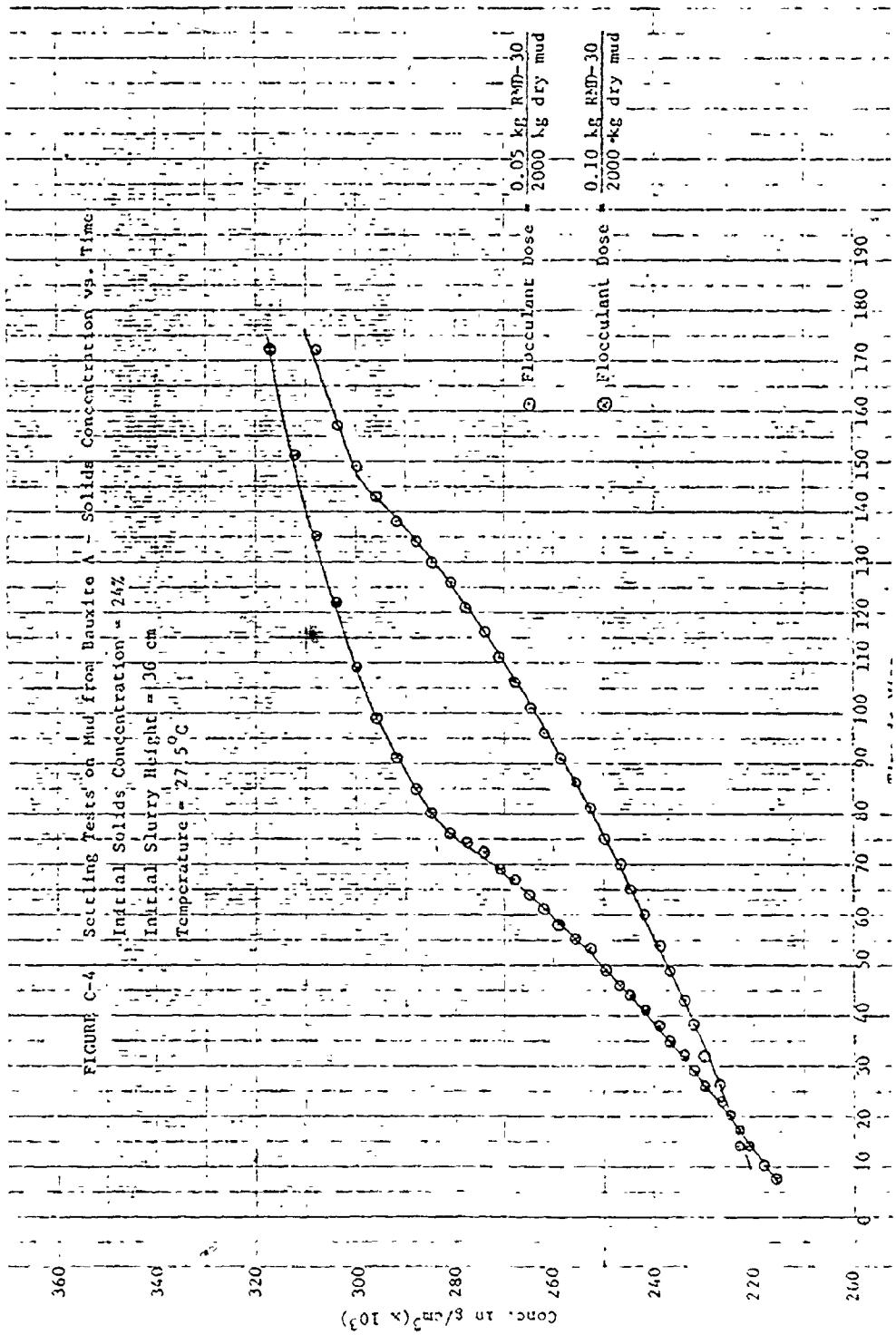

FIGURE C-4 Settling Tests on Mud from Bauxite A — Solids Concentration vs. Time
Initial Solids Concentration = 24%
Initial Slurry Height = 36 cm
Temperature = 27.5°C

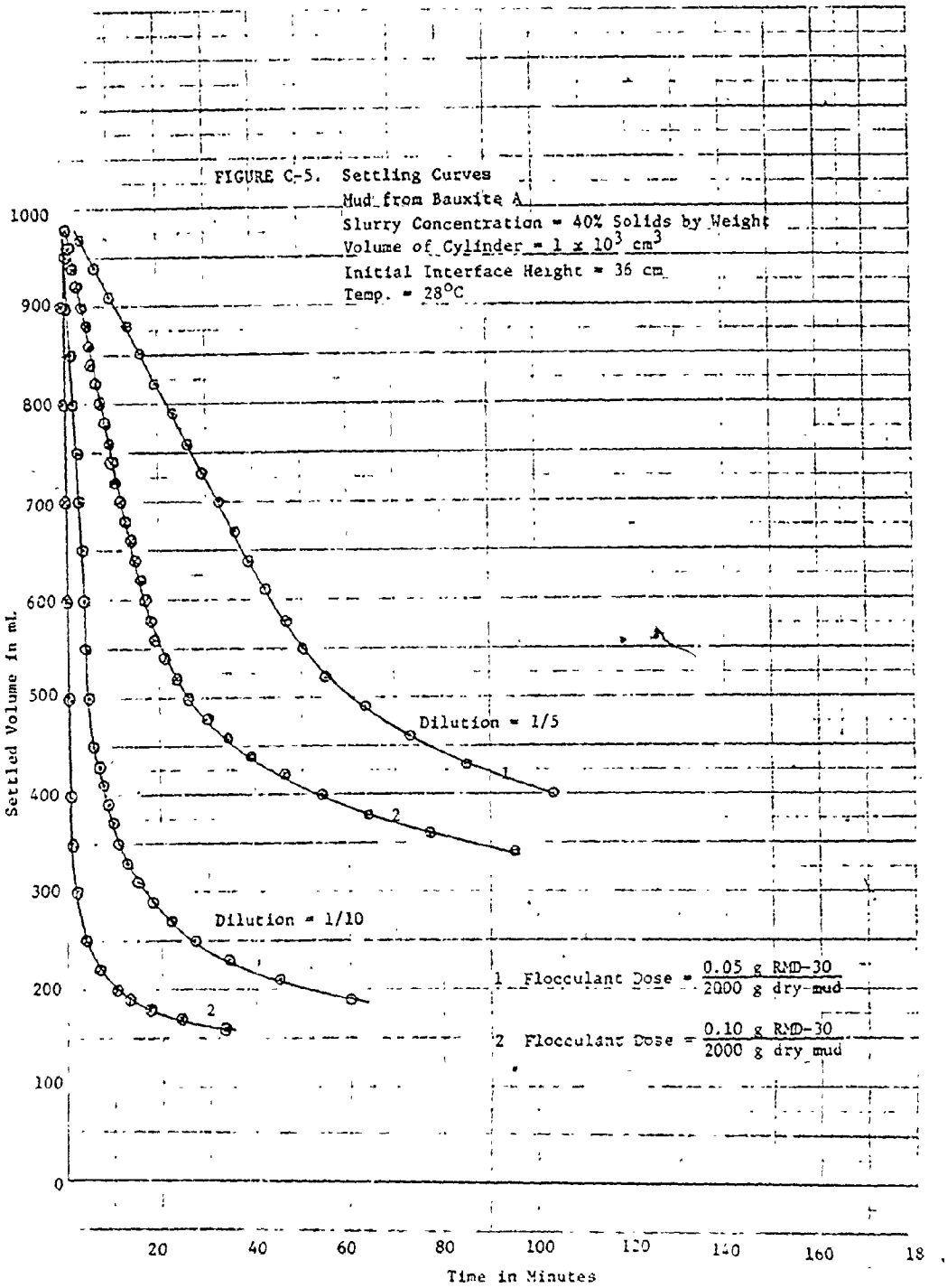

FIGURE C-5. Settling Curves
Mud from Bauxite A
Slurry Concentration = 40% Solids by Weight
Volume of Cylinder = 1×10^3 cm^3
Initial Interface Height = 36 cm
Temp. = 28°C

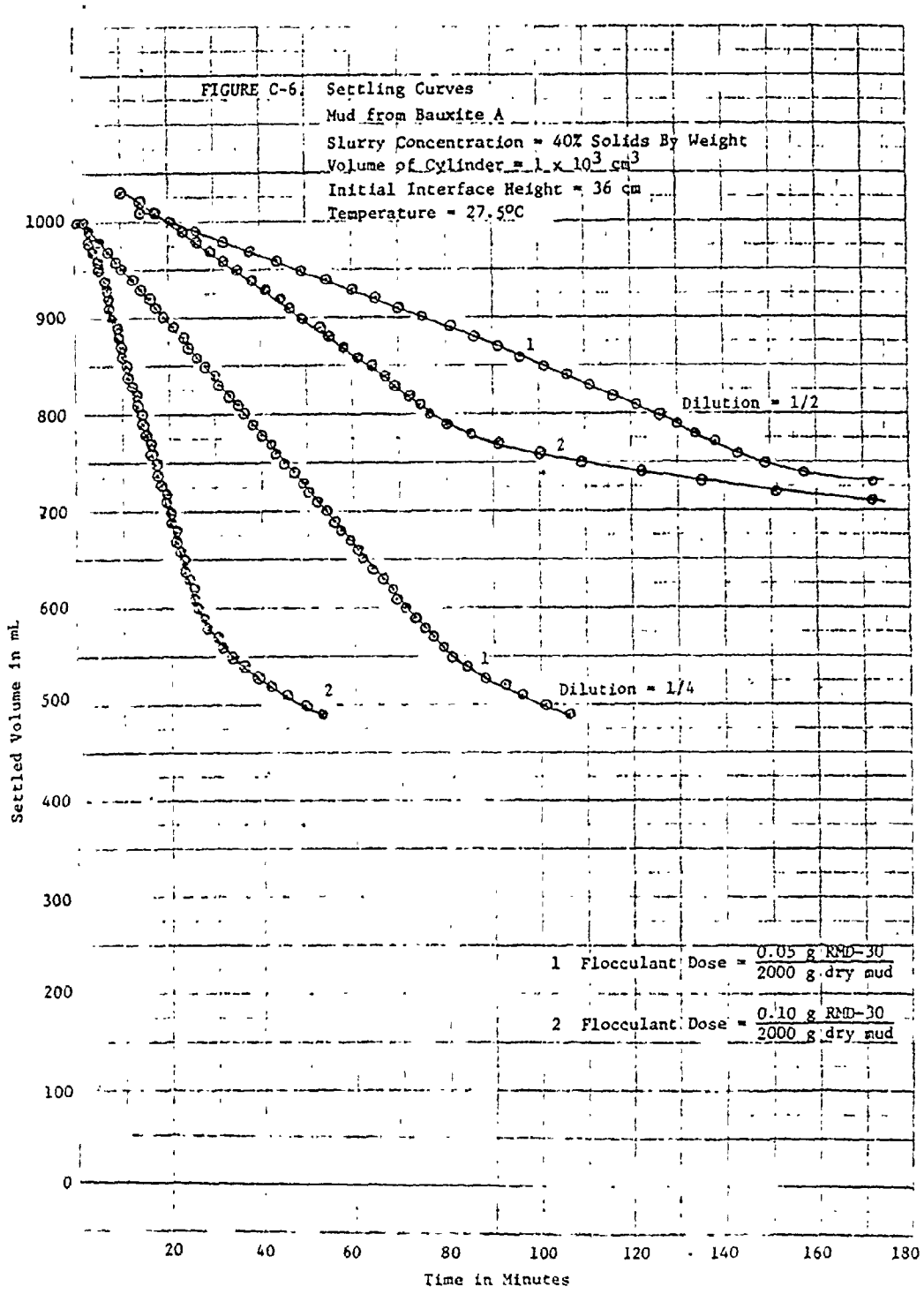
FIGURE C-6. Settling Curves
Mud from Bauxite A
Slurry Concentration = 40% Solids By Weight
Volume of Cylinder = 1 x 10^3 cm^3
Initial Interface Height = 36 cm
Temperature = 27.5°C
Dilution = 1/2
Dilution = 1/4
1
2
1 Flocculant Dose = 0.05 g RMD-30 / 2000 g dry mud
2 Flocculant Dose = 0.10 g RMD-30 / 2000 g dry mud
Settled Volume in mL
Time in Minutes
0
100
200
300
400
500
600
700
800
900
1000
20
40
60
80
100
120
140
160
180

APPENDIX D. Sample Calculations - Run II

D.1 Slurry Feed Rate for Required Throughput

Feed obtained from drums A-2 and A-4.

Solids concentration of slurry feed = 28% = w

Density of liquor in drums = 1.03 g/cm^3 = ρ_l

Density of dried mud = 2.93 g/cm^3 = ρ_s

Using formula from Figure E-1 :

$$\rho_{sl} = \frac{100\ \rho_s \rho_l}{100\ \rho_l + (100 - w)\ (\rho_s - \rho_l)}$$

to calculate slurry density

$$\rho_{sl} = \frac{100 \times 2.93 \times 1.03}{100 \times 1.03 + (100 - 28)\ (2.93 - 1.03)}$$

$$= 1.26 \text{ g/cm}^3$$

For a solids throughput of 1.5 kg/hr ≡ 25 g/min.,

$$\text{Slurry flow rate} = 25 \text{ g } \frac{\text{solid}}{\text{min.}} \quad 1.26 \text{ g } \frac{\text{cm}^3}{\text{slurry}} \quad 0.28 \frac{\text{g slurry}}{\text{g solid}}$$

$$= 71 \text{ cm}^3/\text{min.}$$

Slurry flow rate set at 70 cm^3/min.

Therefore, wash water flow rate = 1.5 x 70 = 105 cm^3/min.

D.2 Synthetic Flocculant (RMD-30) Solution Flow Rate for Desired Dose

Concentration of stock RMD-30 solution = 0.25 g/L

Flocculant dose required = .10 g RMD-30/2000 g dry mud

Therefore, stock solution flow rate

$$= \frac{1000 \text{ cm}^3 \text{ solution}}{.25 \text{ g RMD-30}} \times \frac{25 \text{ g dry mud}}{\text{min}} \times \frac{0.1 \text{ g RMD-30}}{2000 \text{ g dry mud}}$$

$$= 5 \text{ cm}^3 \text{ solution/min}$$

As flow rate of wash water = 105 cm^3/min.,

To every 10^3 cm^3 of distilled water, 50 cm^3 of stock RMD-30 solution is added.

D.3 Mass Balance

Length of column operation = 23 hr

Wash Water

Total volume used = (51-14) + (201-100) L

= 138 L

$$\text{Wash water flow rate} = 138\ \text{L} \times \frac{10^3}{1}\ \frac{\text{cm}^3}{\text{L}} \times \frac{1}{23\ \text{hr}} \times \frac{\text{hr}}{60\ \text{min}}$$

$$= 100\ \text{cm}^3/\text{min}$$

$$= 100\ \text{g/min}$$

Overflow

Quantity of overflow collected ≈ 138 L

Therefore, overflow rate ≈ $100\ \text{cm}^3/\text{min} \times 1.01\ \text{g/cm}^3$

≈ 101 g/min

Underflow (operational 21 hr.)

Quantity of underflow collected ≈ (23.6 + 15 + 14.2 + 13 + 7.0 (samples)) L

≈ 73 L

$$\therefore \text{Underflow rate} = 73\ \text{L} \times \frac{10^3}{1}\ \frac{\text{cm}^3}{\text{L}} \times \frac{1}{21\ \text{hr}} \times \frac{\text{hr}}{60\ \text{min}}$$

$$= 58\ \text{cm}^3/\text{min}$$

$\rho_l = 1.01\ g/cm^3$

$\rho_s = 2.93\ g/cm^3$

$w = 34\%$

$$\rho_{sl} = \frac{100 \times 2.93 \times 1.01}{100 \times 1.01 + (100 - 34)\ (2.93 - 1.01)} = 1.3\ g/cm^3$$

$$\therefore \text{Underflow rate} = 1.3\ \frac{g}{cm^3} \times 58\ \frac{cm^3}{min}$$

$$= 75.4\ g/min$$

$$\approx 75\ g/min$$

Slurry Feed

$$\text{Av. slurry flow rate} = \frac{(70 \times 2) + (69 \times 2) + (65 \times 2) + (66 \times 2) + (65 \times 4) + (66 \times 2) + (64 \times 2) + (66 \times 4) + (64 \times 3.5)}{23.5}$$

$$= 66\ cm^3/min$$

$$\text{Av. \% solids} = \frac{(27.9 \times 13) + (28.4 \times 2) + (27.9 \times 2) + (28.8 \times 2) + (28.5 \times 2) + (29.1 \times 2)}{23}$$

$$= 28.2$$

ρ_s = 2.93 g/cm^3

ρ_l = 1.03 g/cm^3

w = 28%

ρ_{sl} = 1.26 g/cm^3

$$\text{Slurry Feed Rate} = 66 \frac{\text{cm}^3}{\text{min}} \times 1.26 \text{ g/cm}^3 = 83.2 \text{ g/min}$$

$$\approx 83 \text{ g/min}$$

Mass flowing in per minute = 83 + 100 = 183

out = 75 + 101 = 176

$$\text{Corrected solids throughput} = 83 \text{ g/min slurry} \times 0.282 \frac{\text{g solid}}{\text{g slurry}} \times 60 \frac{\text{min}}{\text{hr}}$$

$$= 1.404 \text{ kg/hr}$$

D.4 Calculation of Real (η_{REAL}) and pseudo (η_{PSEUDO}) Separation Efficiencies from Formulae Given in Appendix E-2

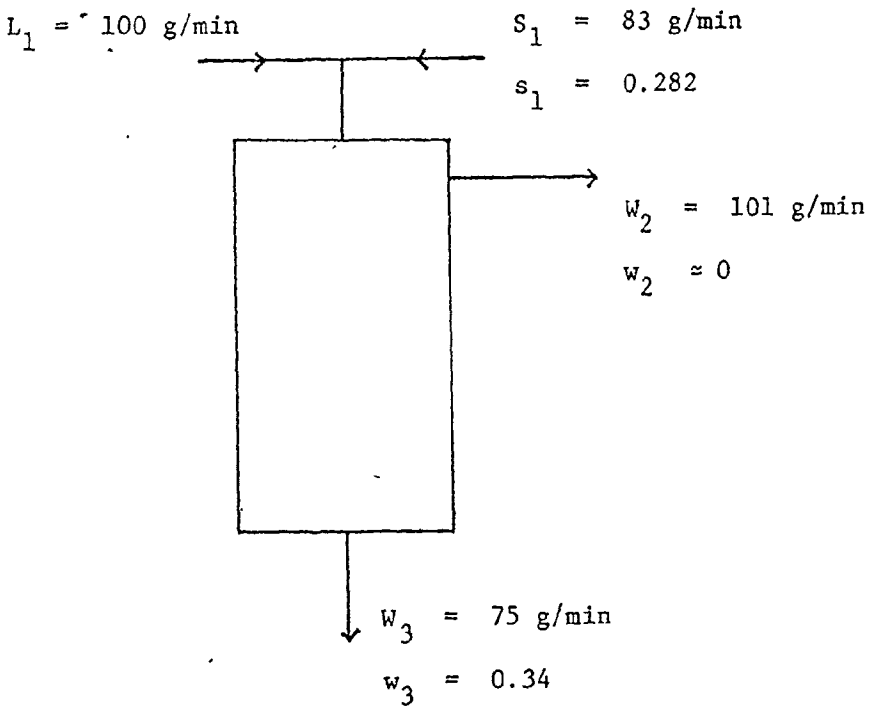

$$W_1 = L_1 + S_1 = 183 \text{ g/min}$$

$$w_1 = \frac{23}{83 + 100} = 0.126$$

$$\eta_{REAL} = \left[\frac{w_3 - w_1}{w_1} \times \frac{W_3}{W_1}\right] 100 = \frac{0.34 - 0.13}{0.13} \times \frac{75}{183} \times 100$$

$$= 66.2\%$$

$$\eta_{PSEUDO} = \left[\frac{w_3 - s_1}{s_1} \times \frac{W_3}{S_1}\right] 100 = \frac{0.34 - 0.28}{0.28} \times \frac{75}{83} \times 100$$

$$= 19.4\%$$

D.5 Calculation of Mixing Efficiency (E_u) from Formulae Given in Appendix E-1

Time weighted average feed T.T.S. concentration

$$= \frac{24.4 \times 2 + 24.1 \times 2 + 24 \times 2}{6}$$

$$= 24.3 \text{ g/L}$$

Average steady state overflow concentration

$$= \frac{11.4 + 11.6 + 11.4 + 10.4 + 10.4 + 10.3}{6}$$

$$= 10.9 \text{ g/L}$$

Average steady state underflow concentration

$$= \frac{8.6 \times 2 + 9.3 \times 2 + 8.6 \times 2 + 9.1}{7}$$

$$= 8.9 \text{ g/L}$$

$$\therefore x_{u,n-1} = 24.3 \frac{\text{g T.T.S}}{\text{L liquor}} \times 10^3 \frac{\text{L}}{\text{cm}^3} \times 1.03 \frac{\text{cm}^3 \text{ liquor}}{\text{g liquor}} = 0.0236 \frac{\text{g T.T.S.}}{\text{g liquor}}$$

$$Xo,n = 10.9 \frac{\text{g T.T.S.}}{\text{L liquor}} \frac{\text{L}}{10^3 \text{ cm}^3} \times 1.01 \frac{\text{cm}^3 \text{ liquor}}{\text{g liquor}} = 0.0108 \frac{\text{g T.T.S.}}{\text{g liquor}}$$

$$xu,n = 8.9 \frac{\text{g T.T.S.}}{\text{L liquor}} \times \frac{\text{L}}{10^3 \text{ cm}^3} \times 1.01 \frac{\text{cm}^3 \text{ liquor}}{\text{g liquor}} = 0.0088 \frac{\text{g T.T.S.}}{\text{g liquor}}$$

$$\therefore E_n = \frac{x_{u'n-1} - x_{u,n}}{x_{u,n-1} - X_{o,n}} \times 100 = \frac{0.0236 - 0.0108}{0.0236 - 0.0088} \times 100 = 86\%$$

where E_n = mixing efficiency

$x_{u,n-1}$ = mass fraction soluble component in the feed

$x_{u,n}$ = mass fraction soluble component in the underflow

$X_{o,n}$ = mass fraction soluble component in the overflow

T.T.S. = total titratable soda

D.6 Synthetic Flocculant Adsorption Efficiency (E_F)

Flocculant dose = 0.10 kg RMD30/2000 kg dry mud

Solids concentration in diluted slurry = 12.7%

$$\text{Concentration of RMD 30 in slurry} = \frac{0.1 \text{ g RMD-30}}{2000 \text{ g dry mud}} \times \frac{12.7 \text{ g dry mud}}{100 \text{ g slurry}}$$

$$= 6.35 \times 10^{-6} \frac{\text{g RMD-30}}{\text{g slurry}}$$

Assuming that all of RMD-30 is initially present in liquor.

Initial RMD-30 concentration in liquor of diluted slurry, F_I,

$$= 6.35 \times 10^{-6} \frac{\text{g RMD-30}}{\text{g slurry}} \times 0.873 \frac{\text{g slurry}}{\text{g liquor}} \times 1.01 \frac{\text{g liquor}}{\text{cm}^3 \text{ liquor}}$$

$$= 7.35 \times 10^{-6} \frac{\text{g RMD-30}}{\text{cm}^3 \text{ liquor}} \times 10^3 \frac{\text{mg}}{\text{g}} \times 10^3 \frac{\text{cm}^3}{\text{L}}$$

$$= 7.3 \frac{\text{mg RMD-30}}{\text{L liquor}}$$

Residual RMD-30 concentration, F_R, = 0.4 mg/L liquor

$$\text{Adsorption efficiency, } E_F, = \frac{(F_I - F_R)}{F_I} \times 100$$

$$= \frac{7.3 - 0.4}{7.3} \times 100 = 94\%$$

APPENDIX E. Definitions, Nomographs, Specifications and Analytical Methods

E.1 Mixing Efficiency Definition

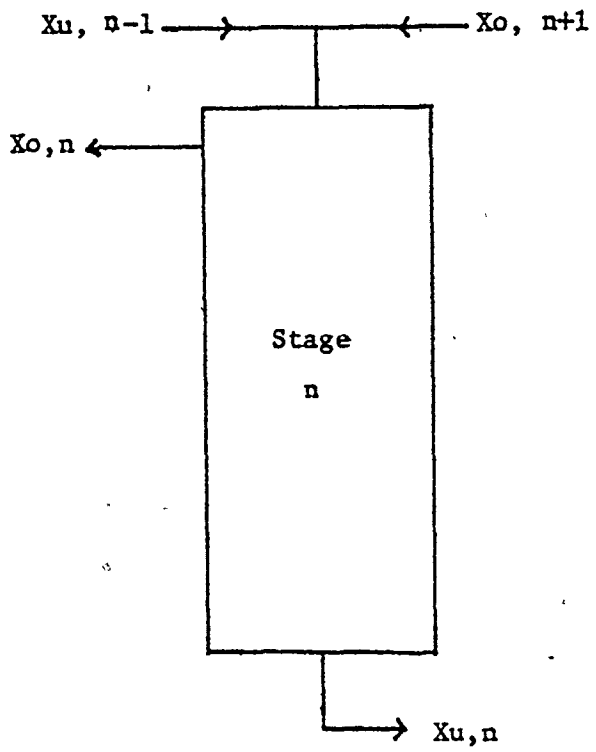

Mixing efficiency, $E_n = \frac{x_{u,n-1} - x_{u,n}}{x_{u,n-1} - x_{o,n}}$

definition from
Scandrett (1963)
page 85

where

E_n = Mixing efficiency of stage n.

$x_{u,n-1}$ = Mass fraction soluble component in the feed to stage n.

$x_{u,n}$ = mass fraction soluble component in the underflow liquid leaving the nth stage.

$X_{o,n}$ = mass fraction soluble component in the overflow from stage n.

$X_{o,n+1}$ = mass fraction soluble component in the wash liquid to stage n.

E.2 Separation Efficiency Definition

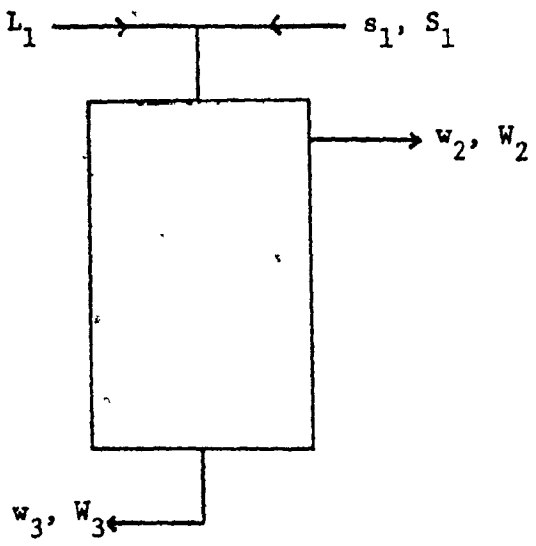

$$\eta_{REAL} = \left[\frac{w_3 - w_1}{w_1} \times \frac{W_3}{W_1} \right] 100$$

$$\eta_{PSEUDO} = \left[\frac{w_3 - s_1}{s_1} \times \frac{W_3}{S_1} \right] 100$$

s_1 = wt. fraction of solid in liquid in slurry

w_1 = wt. fraction of solid in liquid in diluted feed

w_2 = wt. fraction of solid in liquid in overflow

w_3 = wt. fraction of solid in liquid in underflow

L_1 = wash water mass flow rate

S_1 = slurry mass flow rate

W_1 = diluted feed mass flow rate

W_2 = overflow mass flow rate

W_3 = underflow mass flow rate

E.3. Nomograph and Calibration Curves

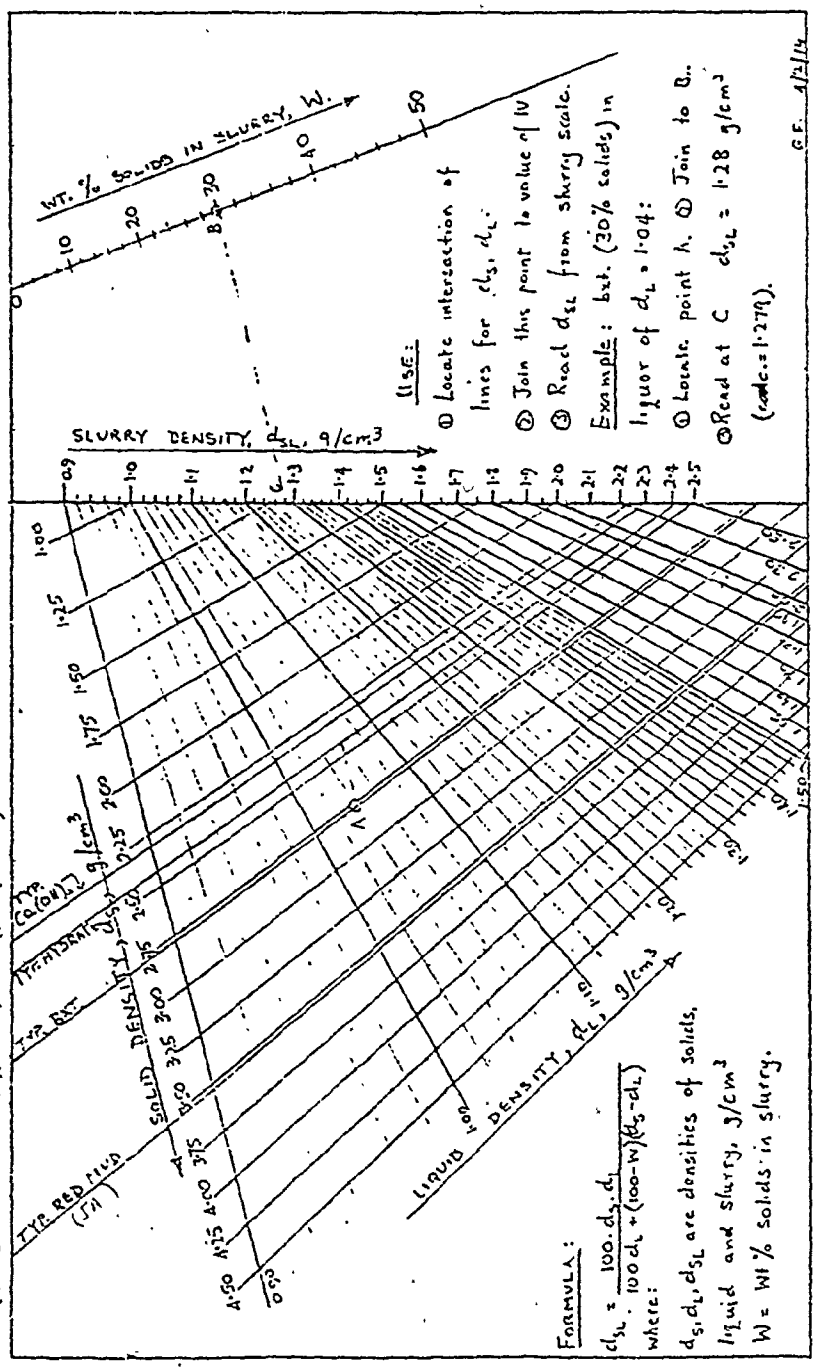
SLURRY DENSITY NOMOGRAPH.
(BASED ON BR. CHEM. ENG., OCT. 1970, P. 1345).
WT. % SOLIDS IN SLURRY, W.
SLURRY DENSITY, d_{SL}, g/cm³
LIQUID DENSITY, d_L, g/cm³
SOLID DENSITY, d_S, g/cm³
TYP. Ca(OH)₂
TYP. RED MUD (SA)
TYP. RED MUD (SA) TREATED
TYP. RED MUD
USE:
① Locate intersection of lines for d_S, d_L.
② Join this point to value of W
③ Read d_{SL} from slurry scale.
Example: bxt. (30% solids) in liquor of d_L = 1.04:
① Locate point A. ② Join to B.
③ Read at C d_{SL} = 1.28 g/cm³
(calc. = 1.279).
FORMULA:
$d_{SL} = \frac{100 \cdot d_S \cdot d_L}{100 d_L + (100 - W)(d_S - d_L)}$
where:
d_S, d_L, d_{SL} are densities of solids, liquid and slurry, g/cm³
W = Wt % solids in slurry.
G.F. 4/21/14

FIGURE E-1

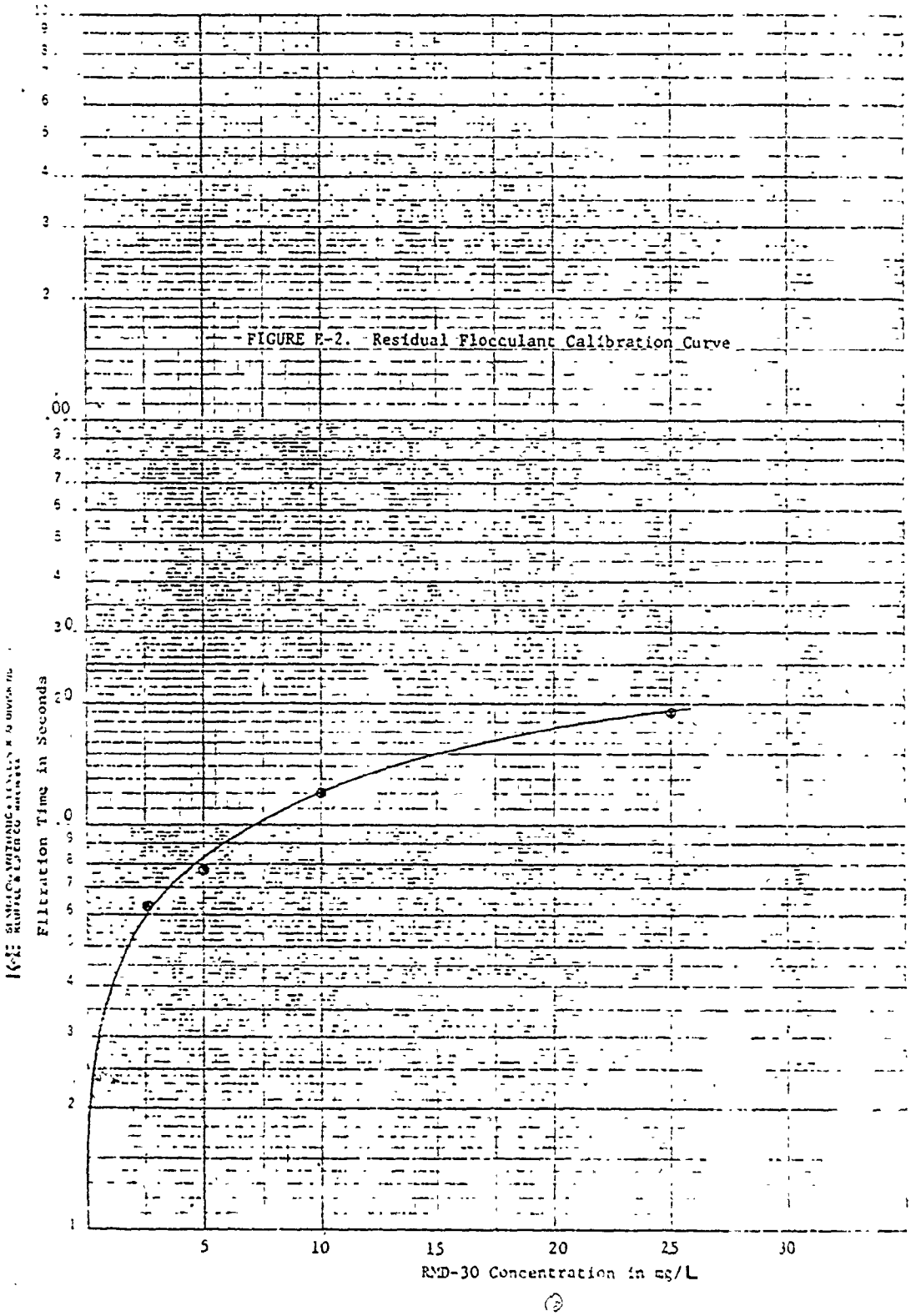

FIGURE E-2. Residual Flocculant Calibration Curve

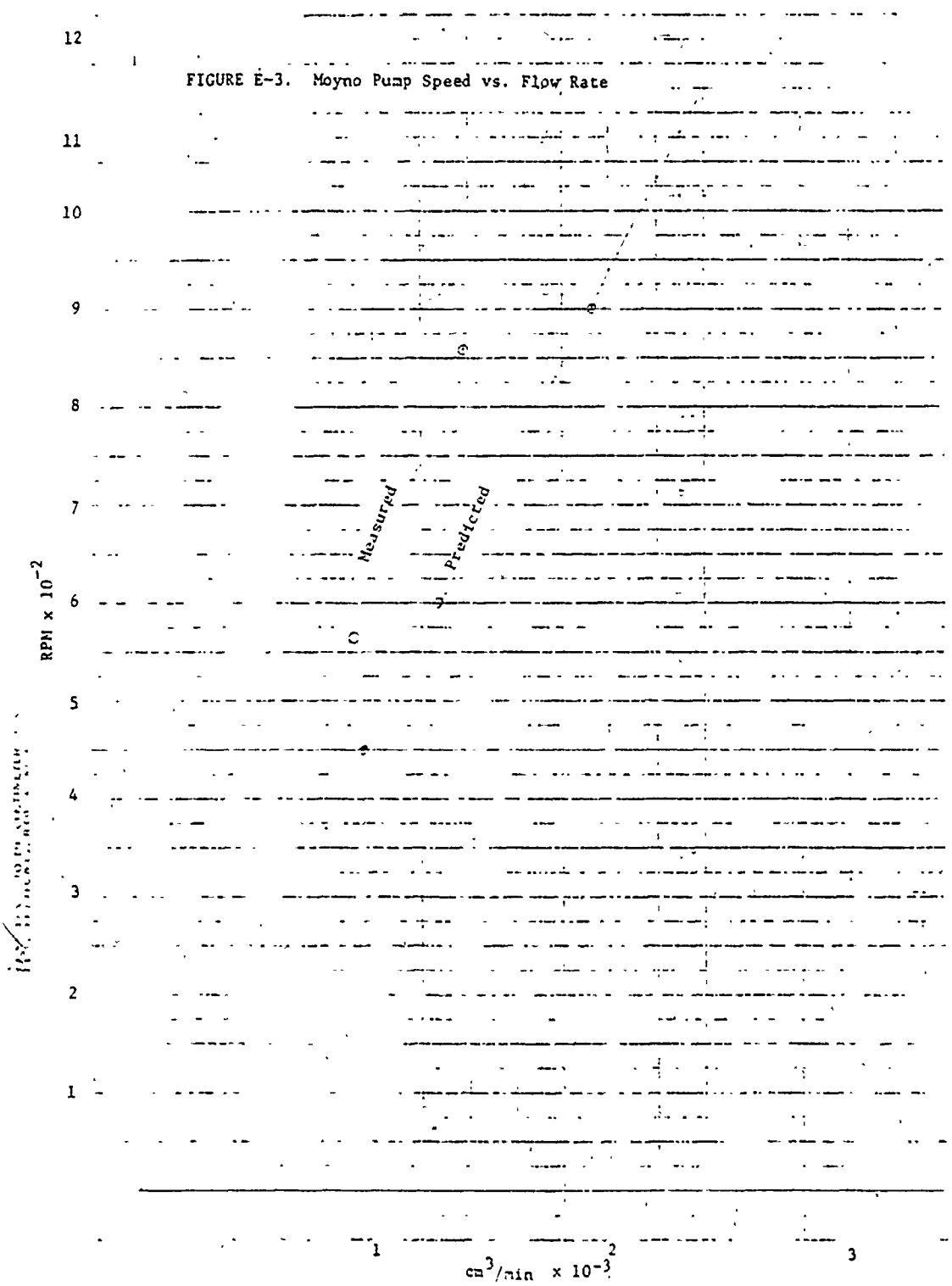

FIGURE E-3. Moyno Pump Speed vs. Flow Rate

E.4. Equipment Specifications

TABLE E-1. Equipment Specifications

Equipment	Specifications	Manufacturer
Mud slurry mixer (Masters Gear-motors)	1/4 H.P., 1725 RPM	Master Electric Co. Mixing Equipment
Wash water mixer (Lightning Mixer)	1/4 H.P., 100/1800 RPM	Mixing Equipment Co. Inc.
Mud slurry feed pump	4-160 mL/min. with pump head #7015	Console Masterflex (Tubing Pump)
Wash water feed pump	4-160 mL/min with pump head #7015	Console Masterflex
Underflow pump (Moyno)	0-2000 cm^3/min. 450 psi - max. press.	Robbins & Myers, Inc. Pump Division
Pump Drive	225 RPM	could not be determined.

E.5. Analytical Methods

TABLE E-2. Analytical Methods Used

Standard Method 57-53:	Determination of solids in liquors and slurries.
Tentative Method 1112-71:	Acidimetric determination of total titratable soda in Bayer plant solutions using sample solutions prepared for thermometric titration analysis.
Standard Method 1111-71R:	Determination of alumina, caustic, and their ratio in Bayer process solutions.
Standard Method 305-61:	Determination of real density or specific gravity of powdered materials pycnometer procedure.
Standard Method 1003-71:	Wet sieve analysis using micromesh sieves.
Standard Method 952-69:	Determination of particle size distribution using an M.S.A. Particle Size Analyzer.
Tentative Method 471-55:	Determination of iron oxide in red mud.
Standard Method 999-69:	Determination of total alumina in red mud.
Tentative Method 472-55:	Determination of Titanium Oxide in red mud.
Tentative Method 468-55:	Determination of silica in red mud.
Tentative Method 467-55:	Determination of loss on ignition of red mud.
Tentative Method 519-69:	Analysis of sulphur dioxide leach solution of red mud for alumina, silica, calcium oxide and soda.